July 2019

Hybrid Fusion Protein for Inhibition of Multiple Proteases for Chronic Wound Healing

Graham L. Strauss
University of South Florida

Hybrid Fusion Protein for Inhibition of Multiple Proteases for Chronic Wound Healing

by

Graham L. Strauss

A thesis submitted in partial fulfillment
of the requirements for the degree of
Master of Science in Biomedical Engineering
Department of Medical Engineering
College of Engineering
University of South Florida

Major Professor: Piyush Koria, Ph.D.
William Lee, Ph.D.
Nathan Gallant, Ph.D.
Mark Jarozeski, Ph.D.

Date of Approval:
June 13, 2019

Keywords: Combination Therapy, Wound Healing, Protease Inhibitor, Recombinant Proteins, Point-Specific Therapy

DEDICATION

I formally dedicate this thesis to my parents for their continued support of my academic pursuits. Also, I dedicate this work to my grandfather, Al Hauptly, as he was a man with an innovative mind, and my observations of his innovative character contributed to the foundation of my ability to use my mind to overcome challenges. Moreover, I thank my extended family and friends for their support. Additionally, I would like to thank my undergraduate advisor and former research mentor, Dr. Terrence Sweeney, for pushing me to pursue a higher education beyond my bachelor's degree. Furthermore, I thank Dr. Janice Voltzow and Mr. Jared Deutsch for their continued professional mentoring throughout my educational career. Most importantly, I thank my twin brother Jonathan for his continued support, and for always motivating me to work towards my fullest potential and reminding me that hard work brings great reward. Lastly, I thank my girlfriend Amanda McCarthy, for her unwavering support; my roommate and friend, Erik May, for his loyalty and selflessness; and my best friend Peter Salerno, who always remains involved in every aspect of my life, even from 1,000 miles away.

ACKNOWLEDGMENTS

First and foremost, I would like to thank Dr. Robert Frisina, for he is a contributor as to why I moved from Pennsylvania to Florida and began pursuing a Master of Science in Biomedical Engineering at USF. From here, I would like to give my utmost gratitude to Dr. Piyush Koria for allowing me the opportunity to volunteer in his lab as a non-degree seeking student and continue in his lab when I matriculated into my master's degree studies. My professional relationship with Dr. Koria has provided me with research skills and guidance that are indispensable as I continue my educational career pursuing my Ph.D. as well as in the future throughout my professional career. Dr. Koria has been one of my greatest mentors as he allowed me his time and attention as I had many questions and curiosities throughout my research. As a professional and superior to me, he gave me the opportunity to question my thoughts, his thoughts, and sit across from each other as two researchers solving a problem together. Additionally, I would like to acknowledge and thank Dr. Tamina Johnson and Tabitha Boeringer as they were integral players involved in my lab training and education in Dr. Koria's laboratory. Lastly, I would like to give my sincerest thanks to a fellow student Chamani Niyangoda for the peer mentoring she provided to me.

TABLE OF CONTENTS

List of Tables iii

List of Figures iv

Abstract vi

Chapter 1: Construction of a Multifunctional Fusion Protein 1
1.1 Introduction 1
1.2 Research Objective 2

Chapter 2: Production and Purification of PMP-D2·ELP·APP-IP 4
2.1 Recombinant Processes Utilizing Microorganisms 4
2.1.1 Inserting PMP-D2 into L10-FLAG pUC19 5
2.1.2 Inserting PMP-D2·L10-FLAG into APP-IP pUC57 6
2.1.3 Inserting PMP-D2·L10-FLAG·APP-IP into pET25b Plasmid 7
2.2 Expression of PMP-D2·L10-FLAG·APP-IP 7
2.3 PMP-D2·L10-Flag·APP-IP Protein Characterization 8
2.3.1 Protein Purification: Inverse Transition Cycling 12
2.3.2 Total Stain Analysis 12
2.4 Inhibitory Activity Analysis of PMP-D2·L10-FLAG·APP-IP 13
2.4.1 Explanation of Inhibition of MMP-2 Assay 14
2.4.2 Explanation of Inhibition of Neutrophil Elastase (NE) Assay 16
2.5 Explanation of Statistical Analysis 17

Chapter 3: PCR Results, Sanger Sequencing, and Western Blot Total Protein Stain for Validation of Recombinant Sequence and the Quality of Protien Purification 18
3.1 Recombinant Process Validation Utilizing PCR and Gel Electrophoresis Throughout the Recombinant Process 18
3.2 Sanger Sequencing Results for Final Validation of the Creation of PMP-D2·L10-FLAG·APP-IP 20
3.3 Validation of Purified PMP-D2·L10-FLAG·APP-IP Utilizing Total Protein Stain Analysis 23

Chapter 4: Dual Activity of PMP-D2·L10-FLAG·APP-IP Inhibiting MMP-2 and Neutrophil Elastase 24
4.1 PMP-D2·L10-FLAG·APP-IP Inhibition of MMP-2 24
4.1.1 PMP-D2·L10-FLAG·APP-IP Compared to the Activity of APP-IP·L10-FLAG 25

4.1.2 PMP-D2·L10-FLAG·APP-IP Compared to the Activity of PMP-D2·L10-FLAG 27
4.1.3 Statistical Significance of MMP-2 Inhibition Data 29
4.2 PMP-D2·L10-FLAG·APP-IP Inhibition of Neutrophil Elastase 30
4.2.1 PMP-D2·L10-FLAG·APP-IP Compared to the Activity of PMP-D2·L10-FLAG 31
4.2.2 PMP-D2·L10-FLAG·APP-IP Compared to the Activity of APP-IP·L10-FLAG 32
4.2.3 Statistical Significance of NE Inhibition Data....33

Chapter 5: Discussion 34

Chapter 6: Future Studies and Applications 37

References....39

LIST OF TABLES

Table 1: Example of the Contents of Each Well Ran in Triplicate for MMP-2 Inhibition 15

Table 2: Example of the Contents of Each Well Ran in Triplicate for NE Inhibition.....17

LIST OF FIGURES

Figure 1 Theory Behind ELP Aggregation and Visual Representation of ELP Behavior During Inverse Transition Cycling 9

Figure 2 Theory Behind ELP Aggregation and Visual Representation of ELP Behavior During Inverse Transition Cycling with the Fusion of a Charged Peptide Region (Yellow Ends) on the End of the ELPs 10

Figure 3 Theory Behind ELP Aggregation and Visual Representation of ELP Aggregation During Inverse Transition Cycling with Fusion of Two Charged Regions at 7.4 pH. 10

Figure 4 Theory Behind ELP Aggregation and Visual Representation of ELP Aggregation During Inverse Transition Cycling with Fusion of Two Charged Regions at pI 11

Figure 5 Transitioning Behavior of PMP-D2‧L10-FLAG‧APP-IP at 7.4 pH and its Isoelectric Point 11

Figure 6 Gel Electrophoresis for Determining Successful Insertion of PMP-D2‧L10-FLAG into APP-IP pUC57 19

Figure 7 Gel Electrophoresis for Determining Successful Insertion of PMP-D2‧L10-FLAG‧APP-IP into pET25b Plasmid. 19

Figure 8 Sanger Sequencing Results for the pET25b Reverse Primer Validating PMP-D2 Sequence Attached to 5’ End of L10-FLAG 21

Figure 9 Sanger Sequencing Results for the pET25b Forward Primers Validating APP-IP Sequence Attached to 3’ FLAG-Tag End of L10-FLAG. 22

Figure 10 Total Protein Stain Analysis Indicating the Purity of the Final Protein After the Inverse Transition Cycling Purification Process. 23

Figure 11 Kinetic Absorbance Measurements Over Time for the Various Concentrations of PMP-D2‧L10-FLAG ·APP-IP to Provide Slopes that Indicate MMP-2 Inhibitory Activity. 25

Figure 12 Kinetic Absorbance Measurements Over Time for the Various Concentrations of APP-IP・L10-FLAG to Provide Slopes that Indicate MMP-2 Inhibitory Activity. 26

Figure 13 Kinetic Absorbance Measurements Over Time for The Various Concentrations of PMP-D2・L10-FLAG Providing Slopes Used to Indicate MMP-2 Inhibitory Activity 28

Figure 14 Percent MMP-2 Inhibition Gained from the Slopes of the Kinetic Readings Across Multiple Concentrations for the Experimental Groups 29

Figure 15 Kinetic Absorbance Measurements Over Time for the Various Concentrations of PMP-D2・L10-FLAG・APP-IP Providing Slopes Used to Indicate NE Inhibitory Activity. 30

Figure 16 Kinetic Absorbance Measurements Over Time for the Various Concentrations of PMP-D2・L10-FLAG Providing Slopes Used to Indicate NE Inhibitory Activity 31

Figure 17 Kinetic Absorbance Measurements Over Time for the Various Concentrations of APP-IP・L10-FLAG Providing Slopes Used to Indicate NE Inhibitory Activity. 32

Figure 18 Percent NE Inhibition Gained from the Slopes of the Kinetic Readings Across Multiple Concentrations for the Experimental Groups 33

Figure 19 From Left to Right: pET25b, LL37・L10-FLAG pET25b, LL37・L10-FLAG・Cecropin-A Transformed into BLR(DE3) E. coli Cells, Respectively 35

ABSTRACT

Many diseases display a multitude of relevant factors that contribute to the persistence of the disease and difficulty treating it. The multifactorial characteristics of some diseases lead to the requirement of combination of treatments in order to restore health. The latter may necessitate the mixing of treatments, medications, and therapeutics to first halt the disease, then assist the human body in returning itself to a state of normality. For example, chronic wounds exhibit this multifactor characteristic in which there exist many factors that lead to the body's inability to properly heal in a timely manner. This presents a further threat to the body, such as exposure to infection and long-term pain. In this example, it is important to look at the ultimate cause of a chronic wound, which may be due to presence of other diseases impairing the body's ability to properly heal. This may include diabetes, initial antibiotic-resistant infection, autoimmune disorders, and poor vasculature. Furthermore, the mentioned causes for chronic wounds may have associations with one another in a single case of a chronic wound. Treating each interrelated cause with drug combinations may run the risk of adverse side effects or further complications due to mixing drugs in a systemic method.

The goal of this study is to develop a point-specific, protein-based therapy that incorporates a single-protein molecule with multifunctional characteristics based on what we know about chronic wounds and infections, as a proof of concept of multifunctional proteins. Multifunctionality of a single therapeutic molecule is desirable because it may eliminate the unknowns of how differing individual chemical or protein therapies may interact when simply

mixed. In addition, examples of peptides, such as antimicrobial peptides, are known to have synergy, and creating a single protein platform that consists of two synergistic peptides could be of value in the making of a protein with greater activity by guaranteeing that the synergistic peptides are local to one another. Furthermore, broad spectrum activity can be obtained by combining two differing peptides.

This proof of concept was accomplished by targeting two proteinases that are upregulated in chronic wounds: Matrix Metalloproteinase-2 (MMP-2) and Neutrophil Elastase. Recombinant DNA techniques were used to create a fusion protein that incorporates an inhibitor of MMP-2, which is a β-Amyloid Precursor Protein-derived Inhibitory Peptide (APP-IP), and PMP-D2, an inhibitor of Neutrophil Elastase. PMP-D2 was joined to the N-terminus of an Elastin-like peptide, while the APP-IP was joined to the C-terminus of the same Elastin-like peptide. Elastin-like peptides (ELPs) are commonly used as a backbone for recombinant protein production as their distinct thermoresponsive characteristics provide adequate protein purification using an inverse transition cycling [3]. In addition, ELPs can serve as point-specific drug delivery platforms with a transition temperature (T_t) near that of normal body temperature causing low diffusivity [3]. Therefore, when ELPs are applied to a site at their T_t, they will aggregate, which provides diffusional limitations of the protein in the application site, and may decrease the reapplication rate needed for a therapeutic, as well as eliminate adverse side effects by retaining the protein to the specific application site.

From this dual fusion, the final resulting protein is PMP-D2·ELP·APP-IP. This protein was tested for its inhibitory activity of both MMP-2 and Neutrophil Elastase. It was hypothesized that the fusion protein, PMP-D2·ELP·APP-IP, would inhibit MMP-2 just as effectively as APP-

IP·ELP unaccompanied by PMP-D2, as well as effectively inhibit Neutrophil Elastase to the same degree as PMP-D2·ELP unaccompanied by APP-IP.

Furthermore, an additional dually fused ELP fusion protein was currently made with two synergistic antimicrobial peptides fused to each end of the ELP. The two antimicrobial peptides used were human-derived LL37 and insect-derived Cecropin A. This novel fusion peptide contains synergistic increase in antibacterial activity in which preliminary data suggests.

CHAPTER 1: CONSTRUCTION OF A MULTIFUNCTIONAL FUSION PROTEIN

1.1 Introduction

Construction of a multifunctional fusion protein allows for a combination therapy utilizing a single molecule. As diseases are very complex and numerous in cause, drug combinations are often needed [6]. Despite multifunctionality, there are other reasons in which drug combinations are used. For example, synergy can be achieved when combining multiple drugs [6, 5]. In relation to peptides, antimicrobial peptides exhibit synergistic interactions increasing their individual activity [7]. Currently, combination therapies are understood as a mixture of drugs or biologics by combining them in a fashion in which each distinct therapeutic exists on its own within a heterogeneous mixture of other distinct components to increase or broaden the therapeutic effect [5]. Peptides in nature offer therapeutic effects like their chemical counterparts. For example, antimicrobial peptides can be used to fight bacterial infection just as common chemical-based antibiotics can be used, although their levels of activity and mechanism may differ, but nevertheless accomplish a similar goal. However, there are downfalls such as their vulnerability to being degraded quickly [2] and their rapid diffusion out of the treatment areas [3], causing the need for an Elastin-like peptide backbone to provide support and low diffusivity [3].

Proteins offer an opportunity that lies in the fact that the DNA that transcribes for them can be easily altered, produced, and applied in different ways that conventional chemical therapeutics cannot. Strategically engineering proteins by harnessing the mechanisms of biology to build recombinant DNA sequences and express them utilizing microorganisms offers an easy method of

creating novel “designer” therapeutics [2]. In respect to multifunctionality, recombinant proteins offer a simple way to construct a molecule with multiple desired therapeutic effects because biotechnology and recombinant technology allows ease of altering DNA sequences [2] and using plasmids and restriction enzymes to cut, splice, and express sequences in microorganisms is a simple plug-and-play procedure. On the other hand, pharmaceutical chemical compounds require extensive chemical reactions to make new molecules which is why it is appealing to simply mix together chemicals to create a heterogeneous compound for multifunctionality, but this method increases possible drug interactions and adverse side effects. On the other hand, despite the ease of novel protein creation, proteins can have undesirable pharmacokinetic parameters [3], as well as unspecific targets due to their various modes of action, such as in the case of antimicrobial peptides, which makes it important to apply proteins and retain them in a specific site [2]. Elastin-like peptides can offer a platform for biologically active peptides to be fused and purified, and in addition, their temperature-dependent aggregation proves useful in controlling their diffusion and keeping them in the site of application [3].

Ease of creating a multifunctional, “designer” protein as one single molecule lends an advantage to consumers that would benefit from keeping a drugs off their list for ingestion by the ability to create proteins that can be applied to medical device surfaces or directly into tissues and observe long term, local retention due to poor diffusional properties. Additionally, it may also appeal to FDA approval in the sense that the protein is a single molecule and a heterogeneous mixture does not provide its multifunctionality.

1.2 Research Objective

This study is directed towards the creation of an ELP fusion protein with dual inhibition of proteinases upregulated in chronic wounds. However, the topic’s applicability in other areas of

disease makes this work a “proof of concept” of the ability to create a multifunctional protein as a single molecule with an ELP backbone for drug delivery. Therefore, another hybrid protein was created that consists of antimicrobial peptides on each end of an ELP. LL37 and Cecropin-A are known to display synergy [7]. The hypothesis was recently made that this overarching molecule could have greater antimicrobial activity than each peptide fused singularly to an ELP because they will be local to each other existing on the same molecule.

In addition, a new strategy for protein purification utilizing pH changes during inverse transition cycling is proposed for increasing protein yield of charged fusion proteins. The pH changes include the addition of the calculated isoelectric point (pI) for the built protein to increase protein aggregation upon heating and hot centrifugation of the protein solution during purification. The isoelectric point neutralizes the dually negatively charged protein molecule, which creates a hypothesis that the change to the pI is a necessary factor to purify ELP fusion proteins with charges located on each side of the ELP.

CHAPTER 2: PRODUCTION AND PURIFICATION OF PMP-D2·ELP·APP-IP

To construct PMP-D2·ELP·APP-IP the specific ELP used to create the fusion protein is L10-FLAG, which is denoted by an amino acid sequence $[(VPGVG)_2(VPGLG)(VPGVG)_2]_{10}$ with a FLAG-tag end used for tracking throughout the purification process via western blotting. APP-IP is a peptide 10 amino acid long sequence denoted by the sequence *ISYGNDALMP*. While the PMP-D2 is a variant consisting of 35 amino acid long sequence denoted by the *EEKCTPGQVKQQDCNTCTCTPTGVWGCTLMGCQPA*. All sequences were ordered in nucleic acid form through GenScript® in an optimized plasmid with additional nucleic acids added to each end of the desired sequences for using specific restriction enzymes, PFLM1 and BGL1, for cutting and obtaining sticky ends to form the nucleic acid sequence to express PMP-D2·L10-FLAG·APP-IP.

2.1 Recombinant Processes Utilizing Microorganisms

L10-FLAG's nucleic acid sequence was created by GenScript® in a pUC19 plasmid, while PMP-D2 and APP-IP nucleic acid sequences were created in a pUC57 plasmid. All plasmids contain a region making them resistant to carbenicillin in order to utilize cloning protocols. The three plasmids were received in a lyophilized form and then dissolved in nuclease-free water following GenScript® preparation protocol. Dilutions of the original solutions of plasmid were diluted by a 1:10 ratio with nuclease-free water. The cloning process is as follows: each plasmid was transformed into E. coli Top10 cells and plated on an agar containing carbenicillin. After a 14-hour incubation in a 37°C incubator, one colony of each plate was placed in 5 ml Terrific Broth

media containing carbenicillin and shaken at 180 rpm in an incubator set at 37°C for 16 to 18 hours. The E. coli was then lysed, and the plasmids were purified using a miniprep kit. After purification, the plasmids were eluted in 30 μL of nuclease-free water and the concentration of each plasmid solution was evaluated using a BioTek® Synergy plate reader and Biotek®'s Gen5 software.

2.1.1 Inserting PMP-D2 into L10-FLAG pUC19

Once plasmid concentrations were found, a single cut in L10-FLAG pUC19 using the restriction enzyme PFLM1 was made yielding a linear DNA sequence. PMP-D2 pUC57 was double cut using restriction enzymes PFLM1 and BGL1, yielding a fragment containing the nucleic acid sequence for PMP-D2 with sticky ends matching the sticky ends for the linear L10-FLAG pUC19. Both the linear L10-FLAG pUC19 and the fragment PMP-D2 was purified using gel electrophoresis on a 0.6% agarose gel (used throughout all processes). The PMP-D2 was separated from other fragments obtained by a double cut of pUC57 plasmid and locating it at a sequence length of 131 base pairs. Both the linear L10-FLAG and PMP-D2 bands were cut out of the gel and dissolved in QG buffer and purified using a miniprep kit. The concentrations of the linear L10-FLAG pUC19 and PMP-D2 fragment was analyzed and a 5:1 fragment to vector ligase reaction was performed splicing the PMP-D2 fragment into a L10- FLAG pUC19 linear segment forming circular plasmids now containing PMP-D2‧L10- FLAG pUC19 and transformed into E. coli Top10 cells plated onto carbenicillin infused agar plate. After a 14-hour incubation, the colonies that formed were isolated and PCR was performed using pUC19 forward and reverse primers. After PCR, each colony was run on gel electrophoresis to identify which colonies contained the desired insert and which were self-ligations by differentiating a desired insert located on a gel at approximately 900 base pairs (PMP-D2‧L10- FLAG nucleic acid sequence length),

while self-ligations will land at 750 base pairs (L10- FLAG nucleic acid sequence length) on the gel. A colony that received the proper plasmid with the insert was isolated and placed in 5 mL of Terrific Broth media plus carbenicillin and incubated in a shaking incubator set at 180 rpm and 37°C for 16 to 18 hours. A mini prep was performed to purify the new plasmid PMP-D2·L10-FLAG pUC19 and was eluted in 30 ul of nuclease-free water and evaluated for its concentration.

2.1.2 Inserting PMP-D2·L10-FLAG into APP-IP pUC57

Next, the previously purified APP-IP pUC57 was linearized using PFLM1, while the newly produced PMP-D2·L10- FLAG pUC19 was double cut using restriction enzymes PFLM1 and BGL1, yielding fragments containing the nucleic acid sequence for PMP-D2·L10- FLAG. The linearized APP-IP pUC57 and PMP-D2·L10-FLAG fragments were isolated using gel electrophoresis and the appropriate bands for the linear strand and fragment were cut from the gel and dissolved in QG buffer, purified using a mini prep, then analyzed for their concentrations

A 5:1 fragment to vector ligation was performed and transformed into E. coli Top10 cells and spread on an agar plate infused with carbenicillin. The plate was incubated for 14 hours in a 37°C incubator. Colonies that formed after the incubation period were isolated, and PCR was performed using pUC57 forward and reverse primers. Then gel electrophoresis was performed to differentiate self-ligations from desired insert plasmids. Self-ligations of APP-IP·L10-FLAG were differentiated by a band landing at 30 bp which is the nucleic acid length of APP-IP, and the proper inserts were found by locating a band at 930 base pairs, which is the length of the nucleic acid sequence for PMP-D2·L10-FLAG·APP-IP. Colonies containing the desired insert was isolated and grown in Terrific Broth media containing carbenicillin, incubated, and shaken at 37°C and 180 rpm, respectively.

2.1.3 Inserting PMP-D2·L10-FLAG·APP-IP into pET25b Plasmid

PET25b plasmid was linearized using the restriction enzyme SFi, while the PMP-D2·L10-FLAG· APP-IP pUC57 was fragmented to obtain the fragment PMP-D2·L10- FLAG· APP-IP using restriction enzymes PFLM1 and BGL1. The linear pET25b plasmid and the PMP-D2·L10-FLAG· APP-IP fragments were purified using gel electrophoresis, miniprepped, and eluted in 30 ul of nuclease-free water. Concentrations of the linear pET25b and the fragment were determined, and a ligation was performed to create a circular plasmid containing the fragment in PET21. Then a transformation was done in E. coli Top10 cells, which were plated on agar infused with carbenicillin and incubated for 14 hours at 37°C. Colonies that grew were isolated and PCR was run using pET forward and reverse primers. Gel electrophoresis was performed to identify colonies that received the proper PMP-D2·L10- FLAG· APP-IP insert by identifying a band at 930 base pairs. A successful insert was identified and placed in Terrific Broth media and incubated overnight for 18 hours. The plasmids were purified performing a miniprep and eluting with 30 ul of nuclease-free water. The plasmids were then confirmed to be PMP-D2·L10- FLAG· APP-IP pET25b by Sanger Sequencing provided by GENEWIZ®.

2.2 Expression of PMP-D2·L10-FLAG·APP-IP

PMP-D2·L10- FLAG· APP-IP pET21 was transformed into E. coli BLR(DE3) competent cells for expression. BLR(DE3) with the PMP-D2·L10- FLAG APP-IP pET25 plasmid allows expression utilizing the T7 promotor of the pET25b plasmid to express the insert sequence. A single colony of the PMP-D2·L10- FLAG APP-IP pET25 in BLR(DE3) inoculated 75 mL of Terrific Broth media with carbenicillin. It was incubated overnight for 18 hours, shaking at 180 rpm, at 37°C, then transferred to 1 liter of Terrific Broth media containing a milliliter of

carbenicillin. The 1-liter culture was incubated overnight for 24 hours, shaking at 180 rpm, at a temperature of 37°C.

2.3 PMP-D2·L10-FLAG·APP-IP Protein Characterization

PMP-D2·L10-FLAG·APP-IP was characterized according to its overall charge and isoelectric point (pI). The protein's isoelectric point is the pH at which the protein has a net charge of zero. Since PMP-D2·L10-FLAG·APP-IP protein is a charged molecule carrying a negative charge on each side of the ELP, this limits the proteins from aggregating at a practical T_t during inverse transition cycling. This is necessary to obtain a yield of protein using inverse transition cycling due to the nature of ELP aggregation, and how negative charges on each side of the neutral ELP will limit the ability of aggregation with repetitive protein molecules. Figure 1 is a representation of the theory behind ELP aggregation during inverse transition cycling. In this figure, an aggregate easily forms when the temperature (T) of the solution rises above the transition temperature (T_t). ELPs interact and stack uniformly when heated beyond T_t. However, in Figure 2, the ELPs fused with a charged peptide now have a region that repel the same regions of the other fusion proteins allowing aggregation, but less interaction due to the repulsive regions.

Figure 3 represents a fusion protein consisting of an ELP centered between two fused charged regions. The hypothesis is that since there is a charge on each end, the proteins will not aggregate upon reaching a T_t making it difficult to purify the proteins using inverse transition cycling. Therefore, characterization of the built fusion protein is necessary to identify a pH at which the protein is at its isoelectric point (pI). Figure 4 displays the hypothesis of what will happen at the proteins' pI and T_t, since the charges are eliminated, the protein aggregation can occur.

The isoelectric point of PMP-D2·L10-FLAG·APP-IP is approximately 4.1 pH. This pH was utilized throughout the purification process, specifically during hot spin cycles of the inverse phase transition cycling. To prove this concept, an experiment was performed. The proteins L10-FLAG and PMP-D2·L10-FLAG·APP-IP were solubilized in 1xPBS then diluted to 0.1 μg/μL in both 7.4 pH 1xPBS and 4.1 pH 1xPBS. Absorbance was measured for each sample in triplicate as well as blanks for both 1xPBS solutions over the series of temperatures 37°C, 42°C, and 50°C. The results show in Figure 5 that L10-FLAG, a neutral control unaffected by pH, transitioned similarly at each pH. However, PMP-D2·L10-FLAG·APP-IP only transitioned when it was at its isoelectric point, 4.1 pH, as seen in Figure 5. This result indicates that the theory on successfully transitioning Elastin-like peptides with two charged ends relies on neutralizing the charges to successfully self-assemble and aggregate out of solution when heated.

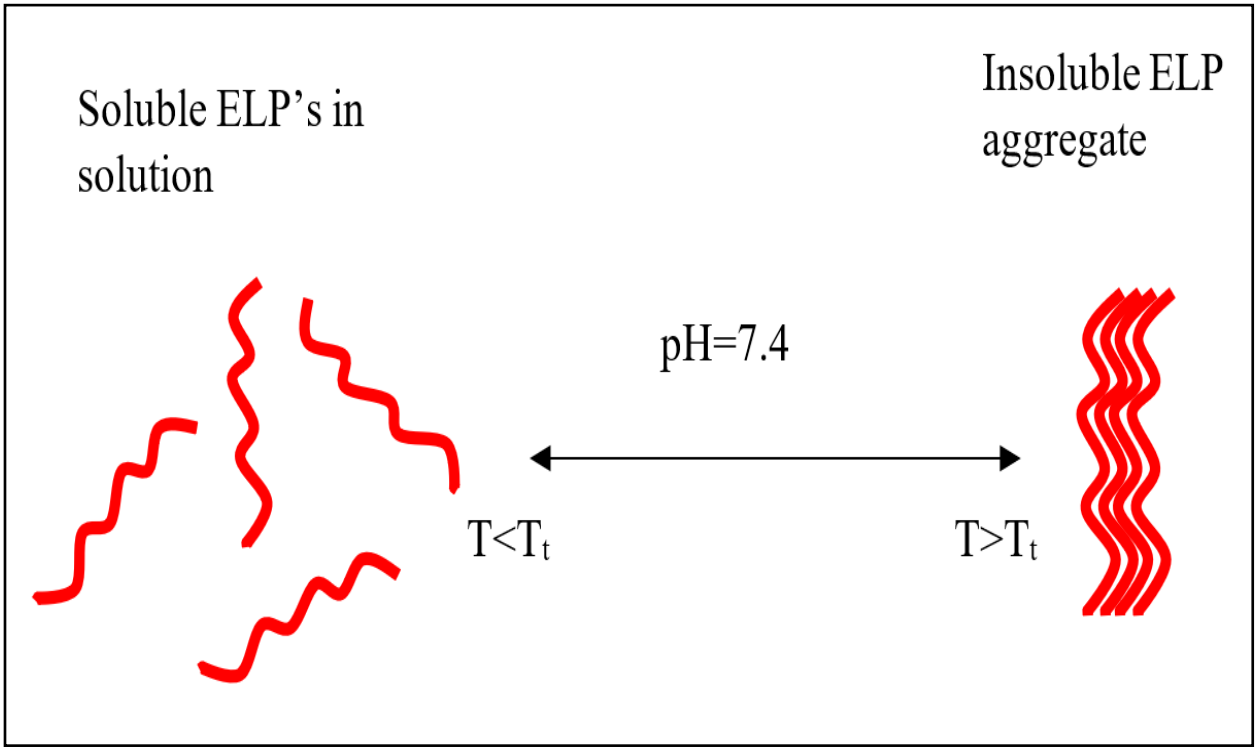

Figure 1 Theory Behind ELP Aggregation and Visual Representation of ELP Behavior During Inverse Transition Cycling

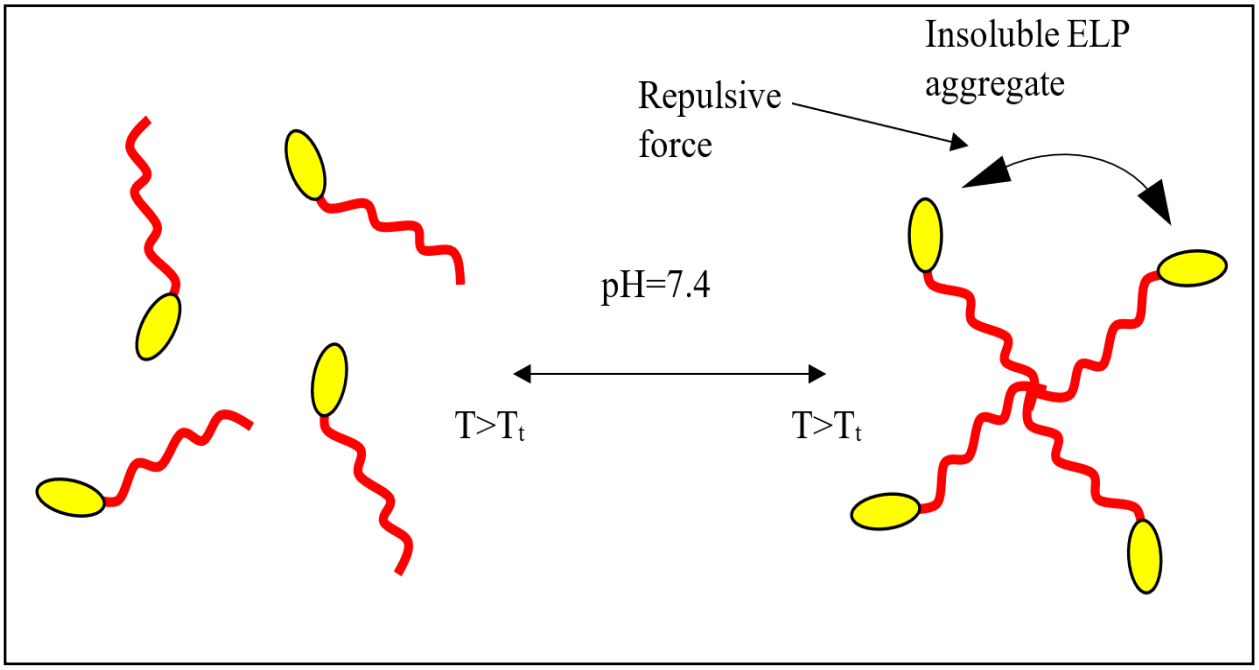

Figure 2 Theory Behind ELP Aggregation and Visual Representation of ELP Behavior During Inverse Transition Cycling With the Fusion of a Charged Peptide Region (Yellow Ends) on the End of the ELPs

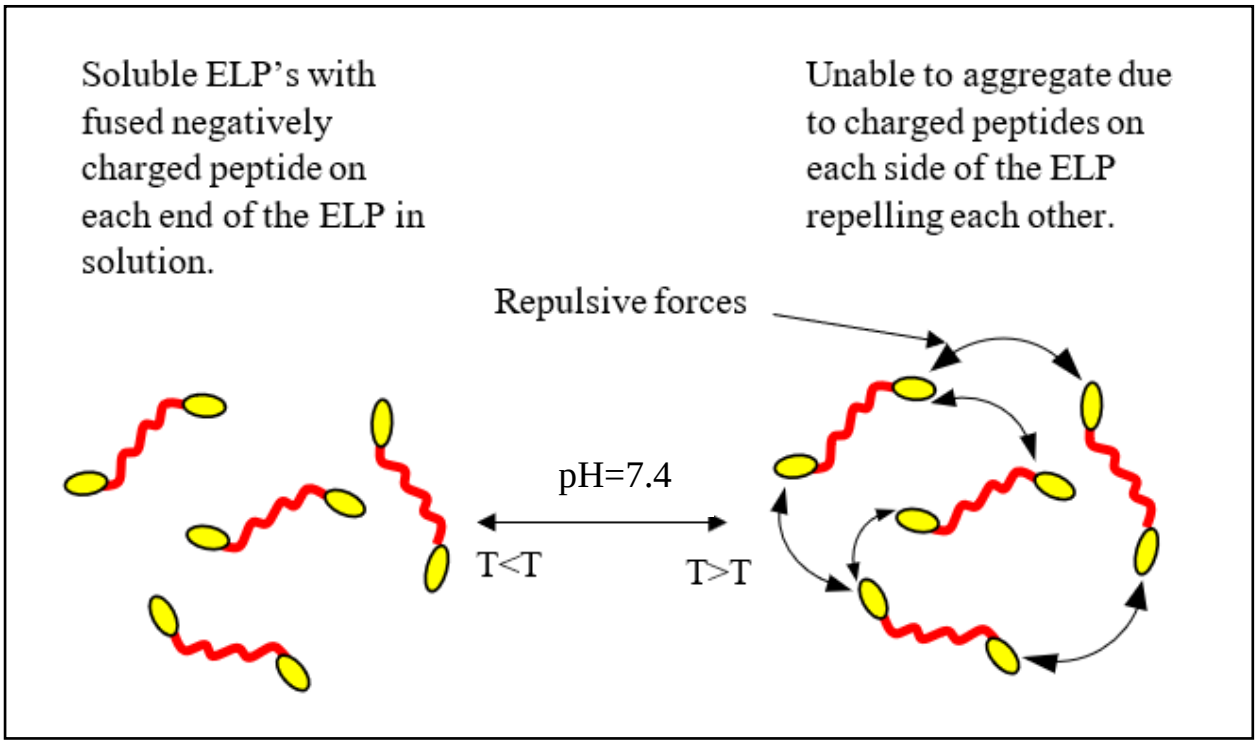

Figure 3 Theory Behind ELP Aggregation and Visual Representation of ELP Aggregation During Inverse Transition Cycling with Fusion of Two Charged Regions at 7.4 pH

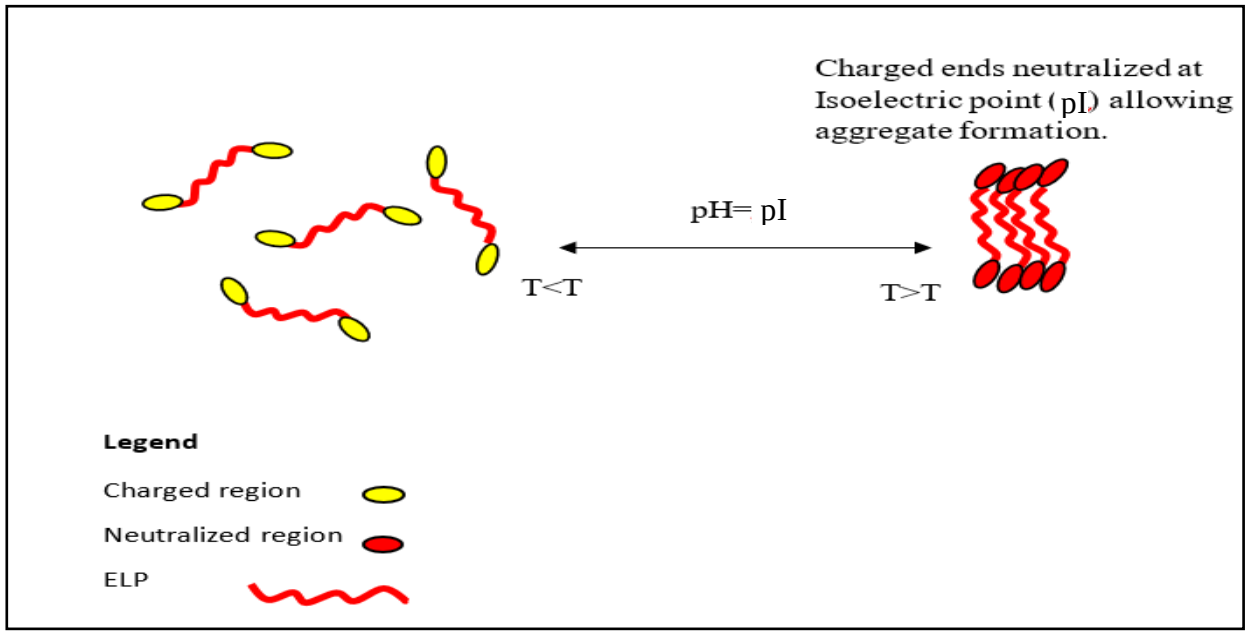

Figure 4 Theory Behind ELP Aggregation and Visual Representation of ELP Aggregation During Inverse Transition Cycling with Fusion of Two Charged Regions at pI

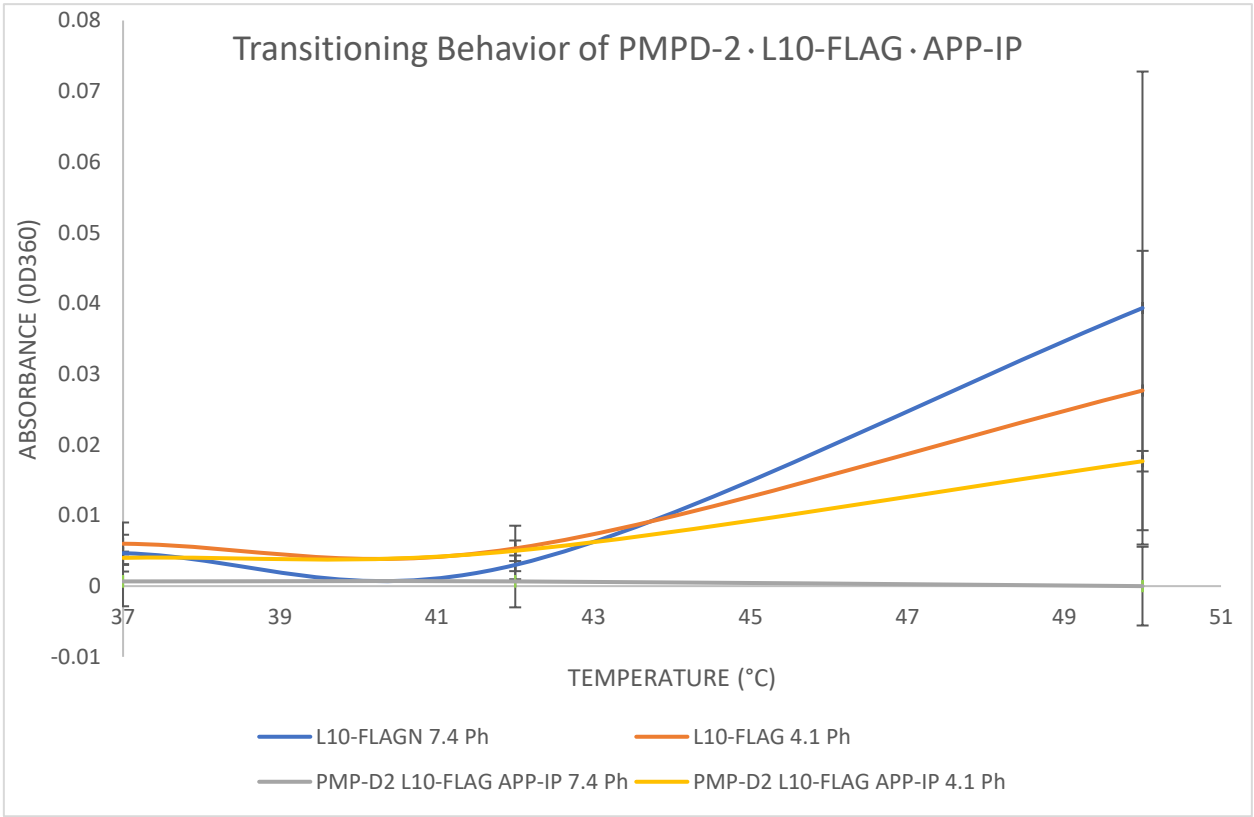

Figure 5 Transitioning Behavior of PMP-D2 · L10-FLAG · APP-IP at 7.4 pH and its Isoelectric Point

2.3.1 Protein Purification: Inverse Transition Cycling

The purification process of this fusion protein is an alteration of the methods used by McCarthy et al [3]. Following a 24-hour incubation period for protein expression, the BLR(DE3) cells were pelleted to remove the cells from the media. The pellet of cells was resuspended in 160 mL of cold 1xPBS. Next, the cells were lysed using several sonication treatments. After lysing the cells, the PMP-D2·L10-FLAG·APP-IP is now soluble in the solution, so the cell lysate was centrifuged at 4°C pelleting out the cell debris leaving PMP-D2·L10-FLAG·APP-IP in solution. After, multiple cold spins removing the cell debris the pH of the protein solution is changed to PMP-D2·L10-FLAG·APP-IP's isoelectric point, 4.1 pH, and salt is added to produce a 4 M NaCl solution to help crash out the protein when heated. The solution was placed in a hot bath of 45°C for 30 minutes (or until the solution turned cloudy, indicating the protein has transitioned). Then the solution is centrifuged at 40°C, ultimately forming a pellet of protein which was then resuspended in 100 mL of cold 7.4 pH 1xPBS until completely resolubilized. Cold spin and hot spin procedures with pH alterations to the pI of PMP-D2·L10-FLAG·APP-IP during the hot spin, were repeated four times to remove any leftover cellular debris and purify the protein. After the final hot spin, the protein pellet was resuspended in 50 mL of cold diH_2O. After a complete resuspension, the pH was ensured to be 7.4 pH and upon full solubilization of the protein, dialysis was performed. Dialysis was performed for 1 hour spinning in fresh diH_2O and then transferred to a fresh drum of diH_2O and left overnight spinning. After 24 hours of dialysis, the 50 mL protein solution was frozen and then lyophilized as the final step of the protein production and purification.

2.3.2 Total Stain Analysis

A total stain analysis was performed on the purified protein and cell lysate to demonstrate the effectiveness of the inverse transition cycling. Total protein staining procedure follows normal

western blotting protocol. However, after the running stage, proteins are not transferred but, the gel is washed and then stained using simple safe blue stain providing an analysis of purity comparing the cell lysate to the final purified product. The protein concentration used for loading was made from a stock of 1 μg/μL then diluted in DTT and 3x red loading buffer making the final protein concentration 0.7 μg/μL. BIO RAD® Precision Plus Protein ™ Kaleidoscope ™ Standard was used for detection of molecular weight of the purified protein upon reading the results of the total protein stain.

2.4 Inhibitory Activity Analysis of PMP-D2·L10-FLAG·APP-IP

Inhibitory action of PMP-D2·ELP·APP-IP was evaluated using Enzo® colorimetric drug discovery kits for both MMP-2 and Neutrophil Elastase. Two additional experimental groups were used for each assay to evaluate the effectiveness of the overarching experimental group PMP-D2·L10-FLAG·APP-IP. The two groups were PMP-D2·L10- FLAG and APP-IP·L10- FLAG. PMP-D2·L10- FLAG was used alongside of APP-IP·L10- FLAG in each assay to display that PMP-D2·L10-FLAG's activity against Neutrophil Elastase, and while APP-IP·L10- FLAG activity in inhibiting MMP-2 is similar to that of the comparing them to the dually fused PMP-D2·L10- FLAG· APP-IP. The results of the two single fusion peptide experimental groups were compared to the results of the dually fused experimental group PMP-D2·ELP·APP-IP to show the dual inhibitory characteristic. Each experiment consisted of groups in triplicate. The experiments included a blank consisting of the assay's buffer, a control with enzyme and substrate in buffer, the experimental groups consisting of the enzymes and their substrates with the possible inhibitory proteins, and blanks containing protein and buffer.

2.4.1 Explanation of Inhibition of MMP-2 Assay

MMP-2 inhibition was tested using Enzo® Life Sciences MMP-2 Colorimetric Drug Discovery Kit. The assay was followed using direct protocol from the kit. This assay is a kinetic assay that consists of an enzyme substrate reaction between MMP-2 and its substrate. The kinetic reading was taken over a 20-minute time interval at an absorbance of 412 nanometers and incubated at 37°C. The control was prepped according to the assay instructions. The final concentrations of protein tested in each well for the experimental groups were 0.004, 0.008, 0.01, 0.05, 0.2, and 0.5 ug/ul. Using the same concentrations, blanks were also run in triplicate, which consisted of each protein in assay buffer to account for any transitioning that may occur due to the temperature parameter of the kinetic experiment. Table 1 represents the four main groups of the experiment and what was placed in each well, as well as what each group was used for. While the mean of the triplicate data for the experimental groups were blanked from the mean of the triplicate data from the associated protein's blank groups. Likewise, was done for the App·L10-FLAG and PMP-D2·L10-FLAG. Based off the means of the triplicate data, the groups were graphed, and their slopes of their trend lines were compared to the negative control to find the 50% inhibitory concentration of the experimental group. The slope of this kinetic assay provides a correlation between the inhibition activity at a specific concentration of protein when compared to the negative control, which will have a steep slope indicating the enzyme substrate reaction is occurring over time, and that slope represents the rate at which this reaction occurs in the presence of no inhibitor. APP-IP·L10-FLAG was compared to the experimental group to analyze if APP-IP was losing, gaining, or remaining the same in activity with the attachment of PMP-D2 to the other end of the L10-FLAG region. Similarly, the data was compared to PMP-D2·L10-FLAG to analyze if it is a contributor to MMP-2 inhibition. The percent inhibition was found by taking the slope of the trend

line for each protein control and experimental control and making it a ratio over the slope of the negative control's trend line then subtracting that value from 1 and multiplying the result by 100. For example, Equation 1 is as follows for the experimental group:

$$\%\, Inhibition = \left(1 - \frac{S_{experimental}}{S_{neg.control}}\right) 100\% \quad (1)$$

where $S_{experimental}$ can be the slope of the experimental groups. $S_{neg.control}$ is the slope of the control containing just the substrate and the enzyme, which is the slope expected when the enzyme substrate interaction occurs with no protein present to inhibit or interfere with the interaction. Therefore, this equation's foundation is a ratio of the slopes of the experimental groups all compared to the slope gained from the measurement of absorbance of the control with an uninterrupted substrate-enzyme interaction. This equation allows for the calculation of percent inhibition in comparison to uninterrupted enzyme substrate interaction.

Table 1 Example of the Contents of Each Well Ran in Triplicate for MMP-2 Inhibition**.**

Group	**Contents**
Blank	Assay Buffer
Control	Assay Buffer+MMP-2+Substrate
PMP-D2・L10-FLAG・APP-IP' (Exp. Group)	Assay Buffer+MMP-2+Substrate+Protein at various concentrations
APP-IP・L10-FLAG (Exp. Group)	Assay Buffer+MMP-2+Substrate+Protein at various concentrations
PMP-D2・L10-FLAG (Exp. Group)	Assay Buffer+MMP-2+Substrate+Protein at various concentrations
Blanks for experimental groups	Assay Buffer+Protein at various concentrations

2.4.2 Explanation of Inhibition of Neutrophil Elastase (NE) Assay

Neutrophil Elastase inhibition was tested using Enzo® Life Sciences Neutrophil Elastase Colorimetric Drug Discovery Kit. The assay was followed using the protocol provided with the kit. This assay is a kinetic assay that consists of an enzyme-substrate reaction between NE and its substrate. The kinetic reading was taken over a 20-minute time interval at an absorbance of 412 nanometers and incubated at 37°C. The negative control was prepped according to the assay instructions. The final concentrations of protein tested in each well for the experimental group and the controls were: $5x10^{-7}$, $5x10^{-6}$, $1x10^{-5}$, and $5x10^{-5}$ ug/ul. Using the same concentrations blanks were run in triplicate, which consisted of each protein in assay buffer to account for any transitioning that may occur due to the temperature parameter of the kinetic experiment. Table 1 represents the 4 main groups of the experiment and what was placed in each well, as well as what each group was used for. The mean of the triplicate data gathered from the negative control was blanked from the mean of the triplicate data gathered from the blank group. While the mean of the triplicate data from the experimental groups was blanked from the mean of the triplicate data from the associated protein blank groups. Based off the means of the triplicate data the groups were graphed and their slopes of their trend lines were compared to the negative control to find the 50% inhibitory concentration of the experimental groups. The slope of this kinetic assay provides a correlation between the inhibition activity at a specific concentration of protein when compared to the negative control, which will have a steep slope indicating the enzyme substrate reaction is occurring overtime, and that slope represents the rate at which this reaction occurs in the presence of no inhibitor. PMP-D2·L10-FLAG was compared to the experimental group to analyze if PMP-D2 was losing, gaining, or remaining the same in activity level with the attachment of APP-IP to the 3’ end of the L10-FLAG region. Similarly, the data was compared to APP-IP·L10-FLAG to

analyze if it is a contributor to NE inhibition. The percent inhibition was found with exact methods from Equation 1 in section 2.4.1.

Table 2 Example of the Contents of Each Well Ran in Triplicate for NE Inhibition.

Group	Contents
Blank	Assay Buffer
Control	Assay Buffer+NE+Substrate
PMP-D2・L10-FLAG・APP-IP (Exp. Group)	Assay Buffer+NE+Substrate+Protein at various concentrations
PMP-D2・L10-FLAG (Exp. Group)	Assay Buffer+NE+Substrate+Protein at various concentrations
APP-IP・L10-FLAG (Exp. Group)	Assay Buffer+NE+Substrate+Protein at various concentrations
Blanks for protein experimental groups	Assay Buffer+Protein at various concentrations

2.5 Explanation of Statistical Analysis

The sample size for each group is N=3 since the experiments were run in triplicate. Each well from the triplicate data for the controls and experimental group were graphed with a trend line providing the estimated slope of the line. Each slope from a set of triplicates were averaged and the standard deviation was found. From the standard deviation, percent standard error was calculated and applied to the percent inhibition data. The standard deviations of the blanks were negated since the blanks oscillate at a very small degree creating a slope near zero

CHAPTER 3: PCR RESULTS, SANGER SEQUENCING, AND WESTERN BLOT TOTAL PROTEIN STAIN FOR VALIDATION OF RECOMBINANT SEQUENCE AND THE QUALITY OF PROTEIN PURIFICATION

Throughout the recombinant process, PCR was performed along with gel electrophoresis to determine successful ligations. Once the final recombinant sequence was inserted into pET25b, the plasmid was sent to GeneWiz® for Sanger Sequencing. After determination of a successful creation of PMP-D2·L10-FLAG·APP-IP in pET25b the protein was expressed and purified. Purification effectiveness was determined using total protein stain analysis.

3.1 Recombinant Process Validation Utilizing PCR and Gel Electrophoresis Throughout the Recombinant Process

The entire nucleic acid sequence of PMP-D2·L10-FLAG·APP-IP has a total length of 911base pairs. After performing the ligation of PMP-D2·L10-FLAG and then the ligation PMP-D2·L10-FLAG·APP-IP PCR and gel electrophoresis was performed to determine which colonies contained the insert, PMP-D2·L10-FLAG·APP-IP versus self-ligations. Figure 6 displays the gel electrophoresis results when PMP-D2·L10-FLAG was inserted into APP-IP pUC57. It is observed in Figure 6 that colony two in lanes 2, and 7-8, received the insert indicated by a high band around 900-1000 base pairs compared to lanes 4 and 10 which have low bands indicating a self-ligation containing just APP-IP, which will fall very low on the gel given the length of 30 base pairs.

The same procedure was done when the insert PMP-D2·L10-FLAG·APP-IP was ligated into pET25b plasmid. In Figure 7, lane 3 indicates a probable ligation specified by the high band

compared to lanes 2 and 4 which show no insert. The colony from lane 3 was selected, grown in culture, and the plasmid was purified for Sanger Sequencing for comprehensive validation.

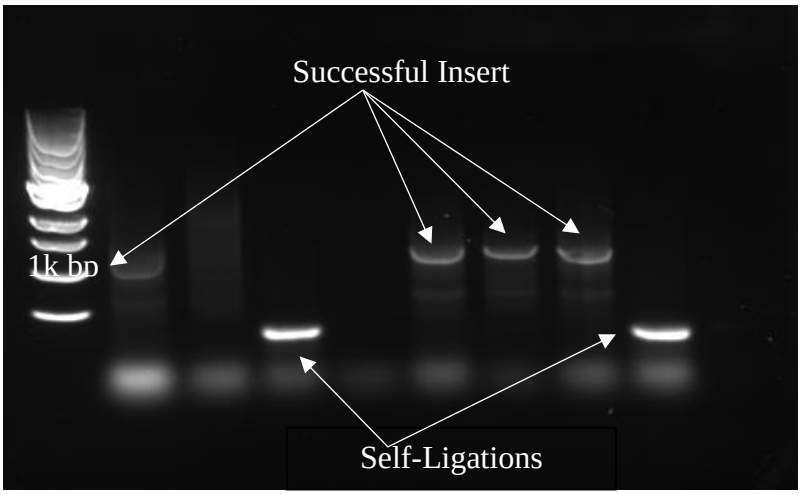

Figure 6 Gel Electrophoresis for Determining Successful Insertion of PMP-D2·L10-FLAG into APP-IP pUC57

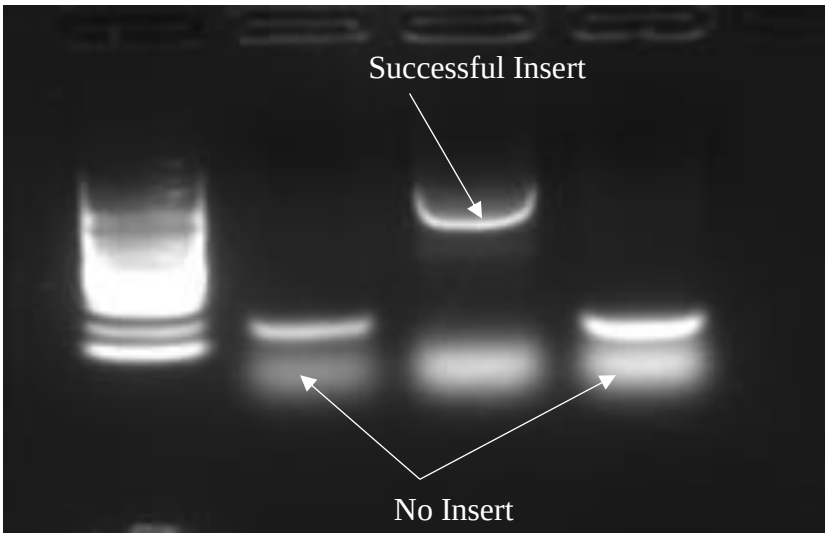

Figure 7 Gel Electrophoresis for Determining Successful Insertion of PMP-D2·L10-FLAG·APP-IP Into pET25b Plasmid

3.2 Sanger Sequencing Results for Final Validation of the Creation of PMP-D2·L10-FLAG·APP-IP

Sanger Sequencing was done through GeneWiz® to validate the final recombinant sequence for PMP-D2·L10-FLAG·APP-IP in a pET25b plasmid. Figure 8 is the result from the Sanger Sequencing. On the left-hand side, PMP-D2 begins the nucleic acid sequence by the amino acid translation *EEKCTPGQVKQQDCNTCTCTPTGVWGCTLMGCQPA* leading into the L10-FLAG region denoted by the 10x repeating *VPGVGVPGVGVPGLGVPGVGVPGVG* (not shown in full in Figure) amino acid translation. On the right-hand side of Figure 9, the Sanger Sequencing shows APP-IP's amino acid translation attached to the FLAG-tag end of L10-FLAG. This validates that the nucleic acid sequence that was built will indeed transcribe for PMP-D2·L10-FLAG·APP-IP.

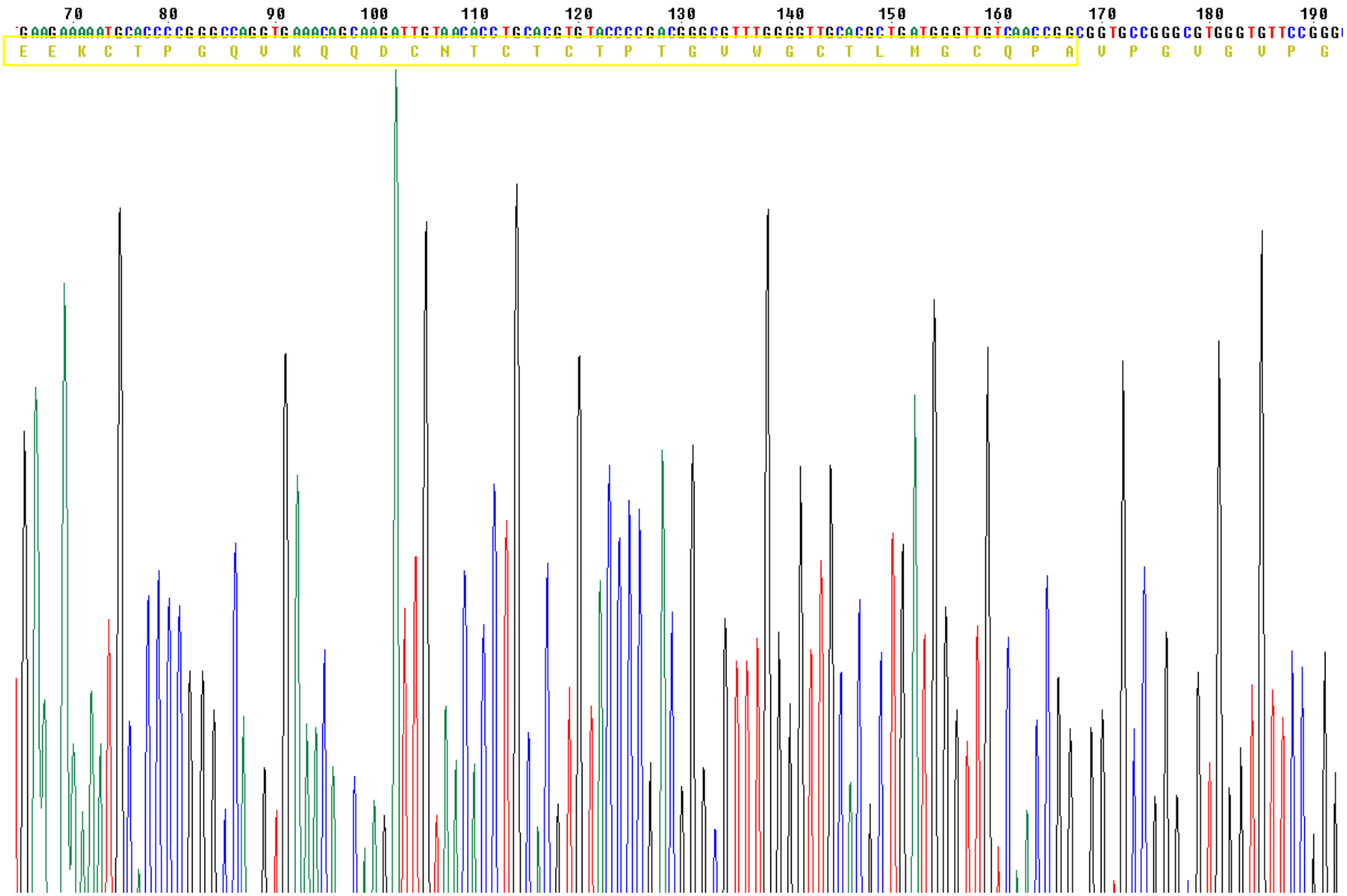

Figure 8 Sanger Sequencing Results for the pET25b Reverse Primer Validating PMP-D2 Sequence Attached to 5' End of L10-FLAG

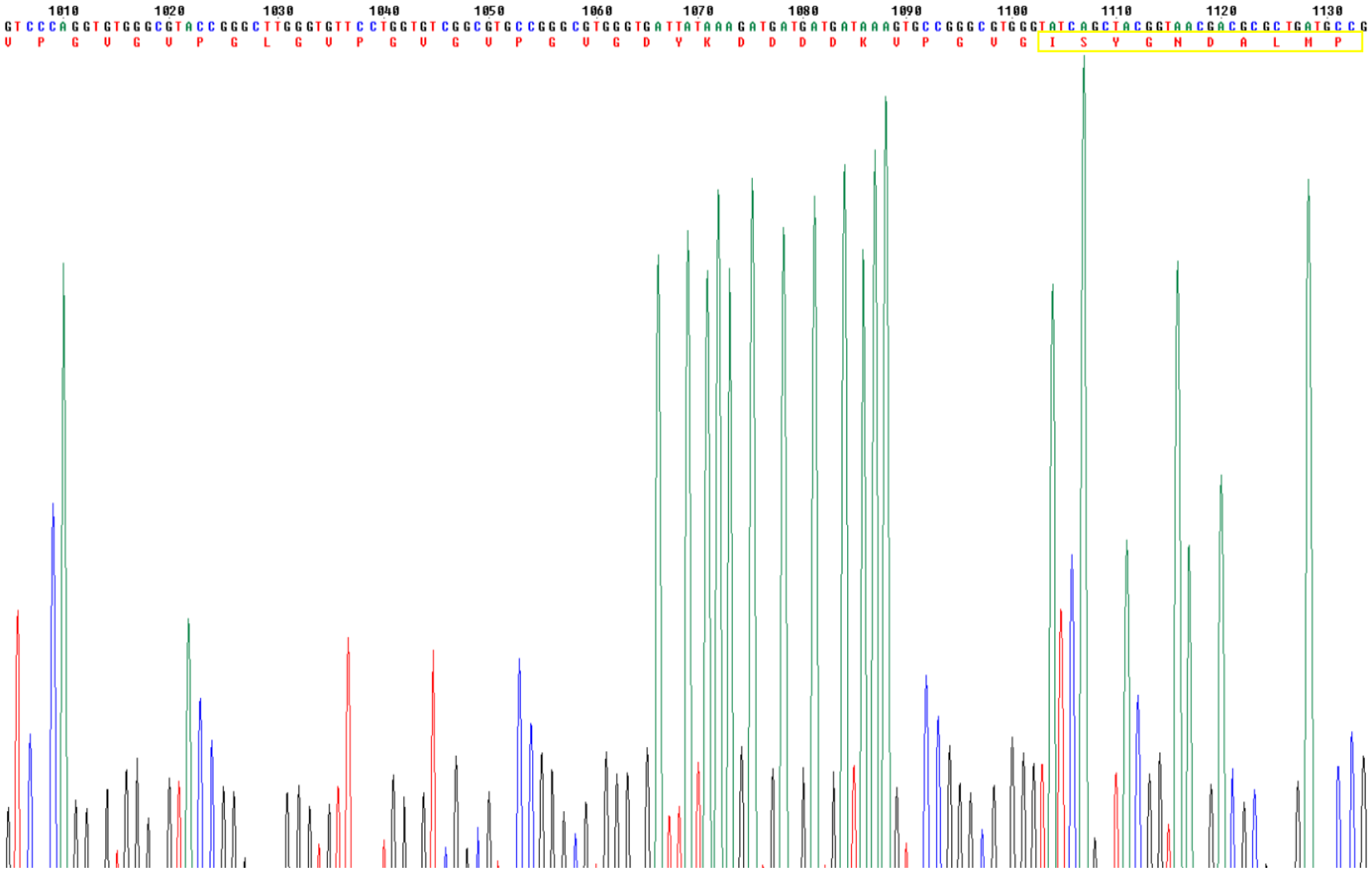

Figure 9 Sanger Sequencing Results for the pET25b Forward Primers Validating APP-IP Sequence Attached to 3' FLAG-Tag End of L10-FLAG

3.3 Validation of Purified PMP-D2·L10-FLAG·APP-IP Utilizing Total Protein Stain Analysis

The total protein stain displays in the first lane, from right to left, the kaleidoscope ladder in Figure 10. The second lane shows the staining of the cell lysate before the protein purification process. The numerous bands are the protein impurities that exist after lysing the cells. The third lane shows the purified final product after 4 cycles of inverse transition cycling.

In the third lane in Figure 10, the final protein, PMP-D2·L10-FLAG·APP-IP, exists as a doublet. A doublet indicates that the protein forms dimers. Additionally, the molecular weight of the purified protein bands center is at the 25 kDa band of the kaleidoscope ladder. This is rational as PMP-D2·L10-FLAG·APP-IP has a calculated molecular weight of 25.396 kDa. The doublet also contains a band between 50 and 75 kDa. This is nearly double the actual weight of the protein further indicating a doublet dimer.

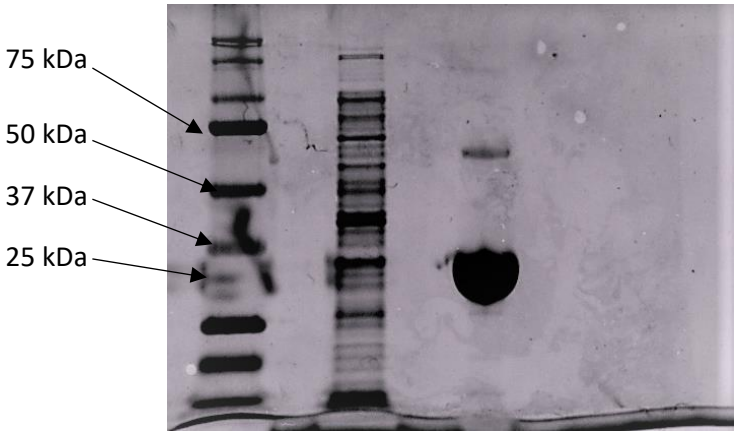

Figure 10 Total Protein Stain Analysis Indicating the Purity of the Final Protein After the Inverse Transition Cycling Purification Process

CHAPTER 4: DUAL ACTIVITY OF PMP-D2·L10-FLAG·APP-IP INHIBITING MMP-2 AND NEUTROPHIL ELASTASE

The activity of PMP-D2·L10-FLAG·APP-IP was evaluated for inhibition of both proteinases, MMP-2 and Neutrophil Elastase. The results of both assays indicate that PMP-D2·L10-FLAG·APP-IP contains inhibition of both MMP-2 and Neutrophil Elastase. While the results indicate activity, they also indicate that no activity was lost by creating a dual inhibitor as one molecule when compared to the results of the singular inhibition proteins, APP-IP·L10-FLAG and PMP-D2·L10-FLAG.

4.1 PMP-D2·L10-FLAG·APP-IP Inhibition of MMP-2

It was observed that PMP-D2·L10-FLAG·APP-IP inhibited the MMP2 enzyme substrate reaction just as well as APP-IP·L10-FLAG. It can be seen in Figure 11 that along varying concentrations of the fusion protein PMP-D2·L10-FLAG·APP-IP, the MMP-2 enzyme substrate reaction was inhibited almost completely at a protein concentration of 0.5 μg/μL. The approximate 50% inhibition concentration was observed at 0.05 μg/μL as indicated in Figure 11 by the light blue line. Using Equation 1, 0.05 μg/μL inhibited MMP-2 at 47.68%. Using the logarithmic trendlines in Figure 13, the equation for the trend line for percent inhibition for PMP-D2·L10-FLAG·APP-IP can be used to calculate 50% inhibitory concentration, which is 0.05 μg/μL as well. The trendline used for this calculation has an R^2=0.99 indicating a very good fit yielding a good approximation of 50% inhibitory concentration.

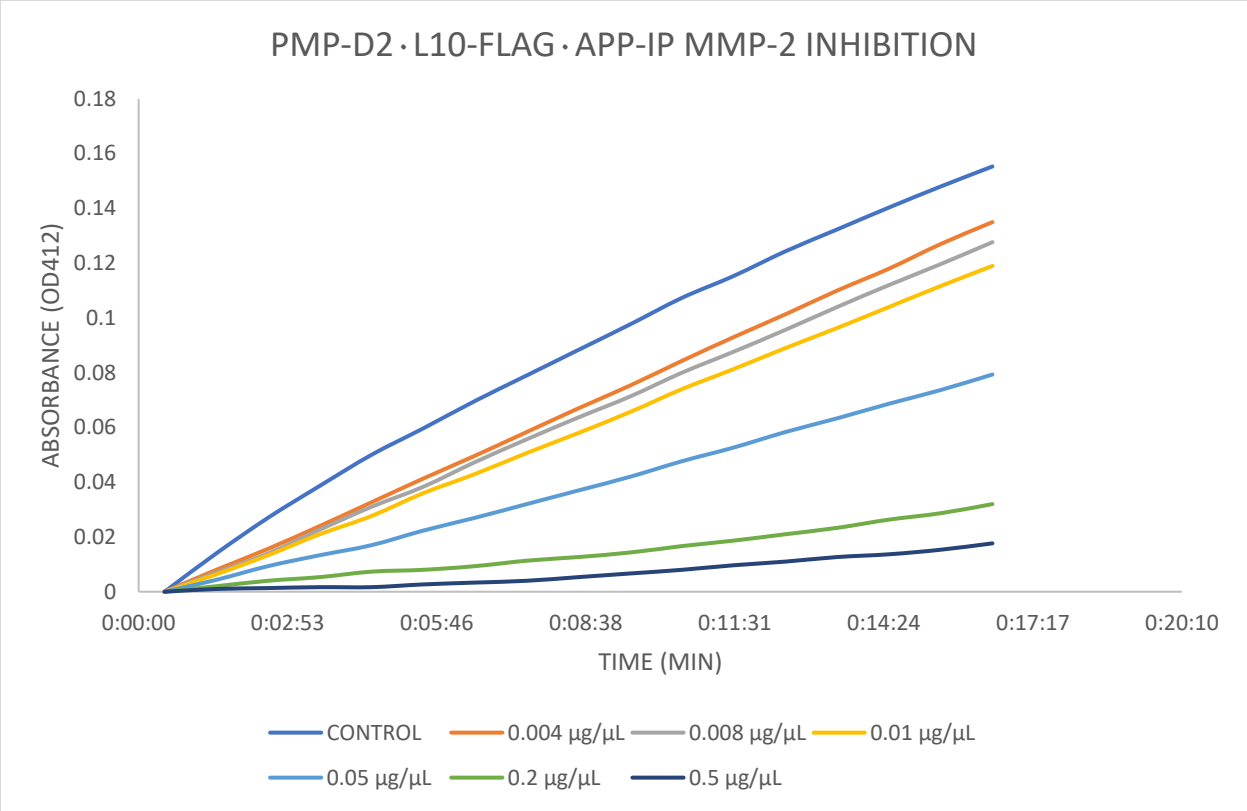

Figure 11 Kinetic Absorbance Measurements Over Time for the Various Concentrations of PMP-D2·L10-FLAG ·APP-IP to Provide Slopes that Indicate MMP-2 Inhibitory Activity

4.1.1 PMP-D2·L10-FLAG·APP-IP Compared to the Activity of APP-IP·L10-FLAG

APP-IP·L10-FLAG inhibited the MMP-2 enzyme substrate interaction. As seen in Figure 12, 0.05 µg/µL APP-IP·L10-FLAG obtained approximately 50% inhibition, which is like what was seen with PMP-D2·L10-FLAG·APP-IP and expected since APP-IP is the MMP-2 inhibitory protein of the overarching fusion protein. Using Equation 1, the slopes of trendlines for the curves in Figure 12 the exact observed percent inhibition of MMP-2 for 0.05 µg/µL APP-IP·L10-FLAG was 46.45%. This indicates that PMP-D2·L10-FLAG·APP-IP inhibits MMP-2 at the same level as APP-IP·L10-FLAG, suggesting that the additional fusion of PMP-D2 to make PMP-D2·L10-FLAG·APP-IP did not affect APP-IP's ability to inhibit MMP-2. The trend line found in Figure 13 provided an equation that yields a calculated 50% inhibitory concentration of 0.04 µg/µL, with the trend line being a good fit indicated by a R^2=0.95. The strong R^2 indicates a reliable estimation

of the 50% inhibitory concentration for APP-IP·L10-FLAG. With PMP-D2·L10-FLAG·APP-IP and APP-IP·L10-FLAG calculated 50% inhibitory concentrations being .04 and .05 µg/µL respectively, it can be concluded that PMP-D2·L10-FLAG·APP-IP inhibits MMP-2 just as effective as singular APP-IP·L10-FLAG. This indicates that the additional fusion of PMP-D2 does not subtract inhibitory power of APP-IP on the fusion protein PMP-D2·L10-FLAG·APP-IP.

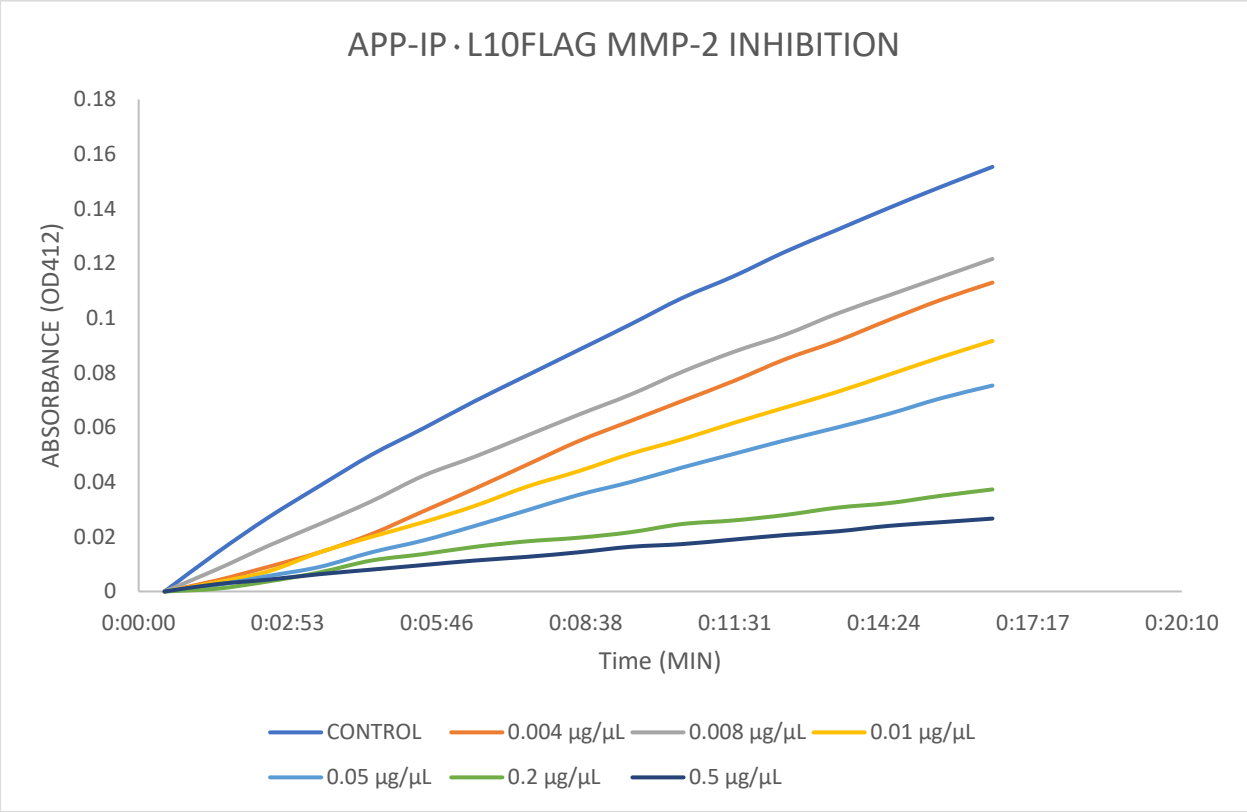

Figure 12 Kinetic Absorbance Measurements Over Time for the Various Concentrations of APP-IP·L10-FLAG to Provide Slopes that Indicate MMP-2 Inhibitory Activity

4.1.2 PMP-D2·L10-FLAG·APP-IP Compared to the Activity of PMP-D2·L10-FLAG

It is expected that PMP-D2·L10-FLAG will have little effect on inhibiting MMP-2. Figure 5 displays the MMP-2 inhibition across the different PMP-D2·L10-FLAG concentrations. It is observed that at its highest concentration tested, which was 0.5 μg/μL, inhibition was near 50%. Using Equation 1 and the slopes of the trend lines obtained from the curves in Figure 13, it was observed that 0.5 μg/μL inhibited MMP-2 activity by 47.34%. Despite the observation of inhibition of MMP-2 by PMP-D2·L10-FLAG, the approximate 50% inhibition concentration was larger by a factor of 10 when compared to the experimental groups PMP-D2·L10-FLAG·APP-IP and the APP-IP·L10-FLAG. Figure 14 represents the percent inhibition curves for the experimental group versus singularly fused proteins. From Figure 14 it is observed that PMP-D2·L10-FLAG nearly levels off at 50% inhibition at 0.5 μg/μL. However, the experimental group, PMP-D2·L10-FLAG·APP-IP shows nearly 90% inhibition of MMP-2 at 0.5 μg/μL. Furthermore, the APP-IP·L10-FLAG shows to only inhibit MMP-2 at 82% inhibition. This small difference can be seen in Figure 13 and leads to the question that PMP-D2 may add to the effective inhibition of MMP-2 for the fusion protein, PMP-D2·L10-FLAG·APP-IP. However, the conclusion is that APP-IP contains majority of the MMP-2 inhibitory properties for the fusion protein PMP-D2·L10-FLAG·APP-IP, as it has very similar percent inhibition values compared to APP-IP·L10-FLAG, but PMP-D2 may contribute some inhibitory activity as well.

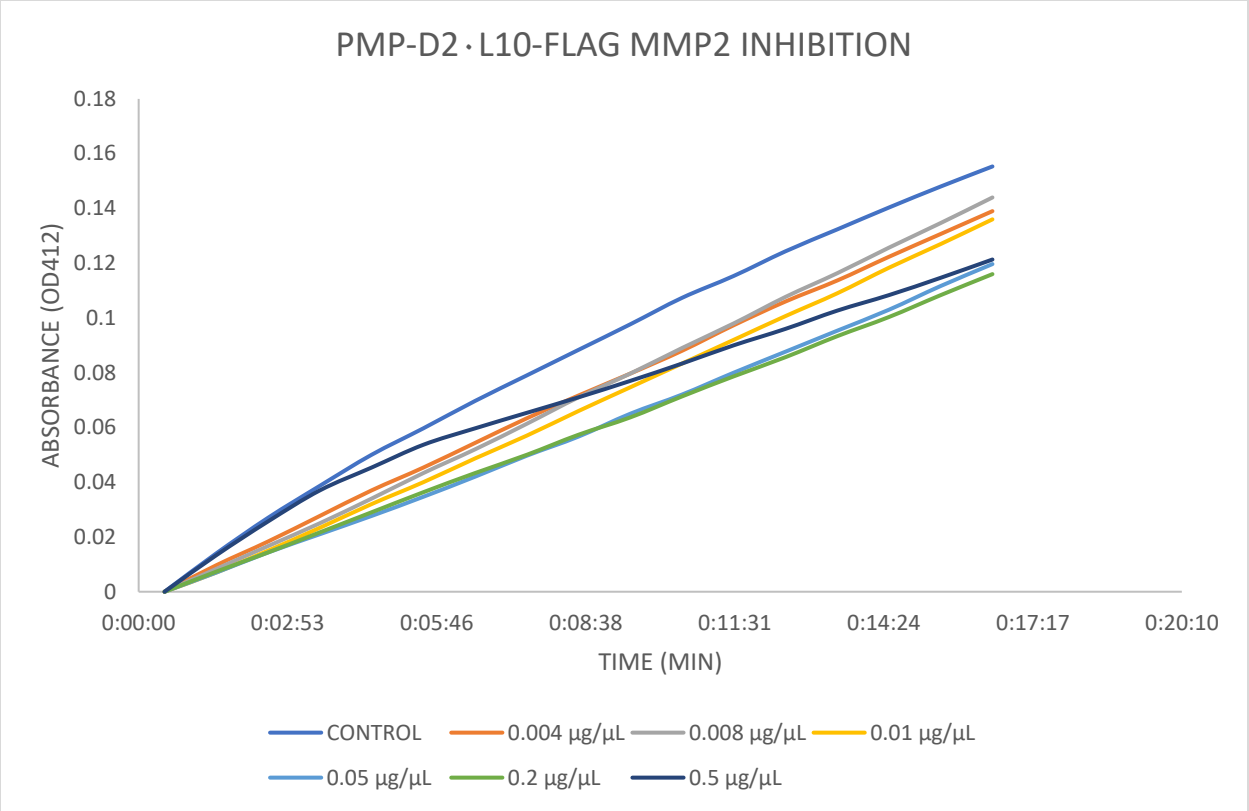

Figure 13 Kinetic Absorbance Measurements Over Time for the Various Concentrations of PMP-D2·L10-FLAG Providing Slopes Used to Indicate MMP-2 Inhibitory Activity

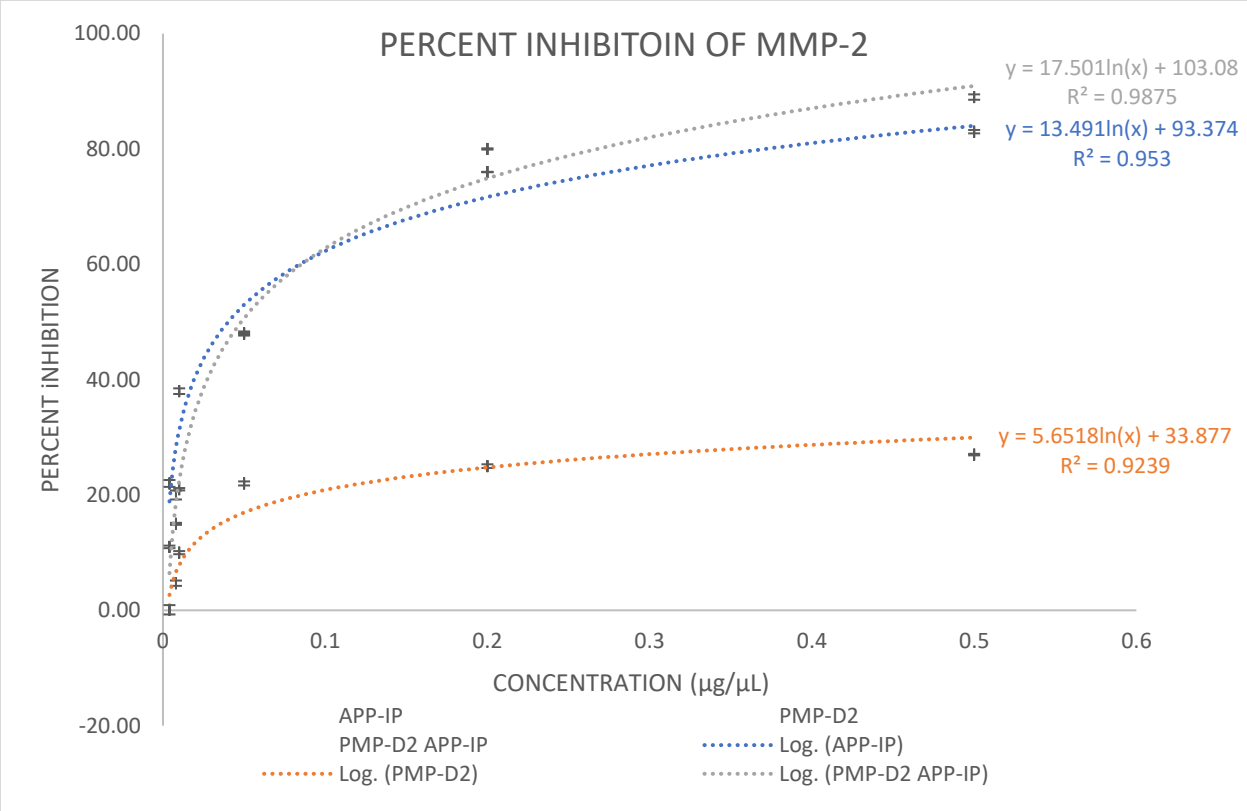

Figure 14 Percent MMP-2 Inhibition Gained from the Slopes of the Kinetic Readings Across Multiple Concentrations for the Experimental Groups

4.1.3 Statistical Significance of MMP-2 Inhibition Data

The statistical significance of the calculations of 50% inhibitory concentration is strong with $R^2 \geq 0.89$ indicating the trendlines used for the calculations of 50% inhibitory concentrations are a good fit and calculations based off the trend lines are rational. Also, percent standard error was found for the percent inhibition, which can be viewed on Figure 14. It can be observed that the standard error is small. Furthermore, N=3 and with a larger N, the standard error would decrease even more since the results seen are very repeatable. Throughout the process of locating an array of inhibitory concentrations, for some concentrations, there existed other data that is not included in order to keep N the same across all experiments, but that additional data shows consistency.

4.2 PMP-D2·L10-FLAG·APP-IP Inhibition of Neutrophil Elastase

PMP-D2·L10-FLAG·APP-IP contained activity against Neutrophil Elastase as seen in the NE inhibition assays. In fact, PMP-D2·L10-FLAG·APP-IP was effective at inhibiting NE at extremely low concentrations when compared to the MMP-2 inhibition. This can be observed in Figure 15, which displays the inhibition activity of PMP-D2·L10-FLAG·APP-IP at various concentrations compared to the control. The near 50% inhibitory concentration was observed between $5x10^{-6}$ and $1x10^{-5}$ µg/µL. Using the logarithmic trendline from Figure 19 the estimated 50% inhibitory concentration is $8.5x10^{-7}$.

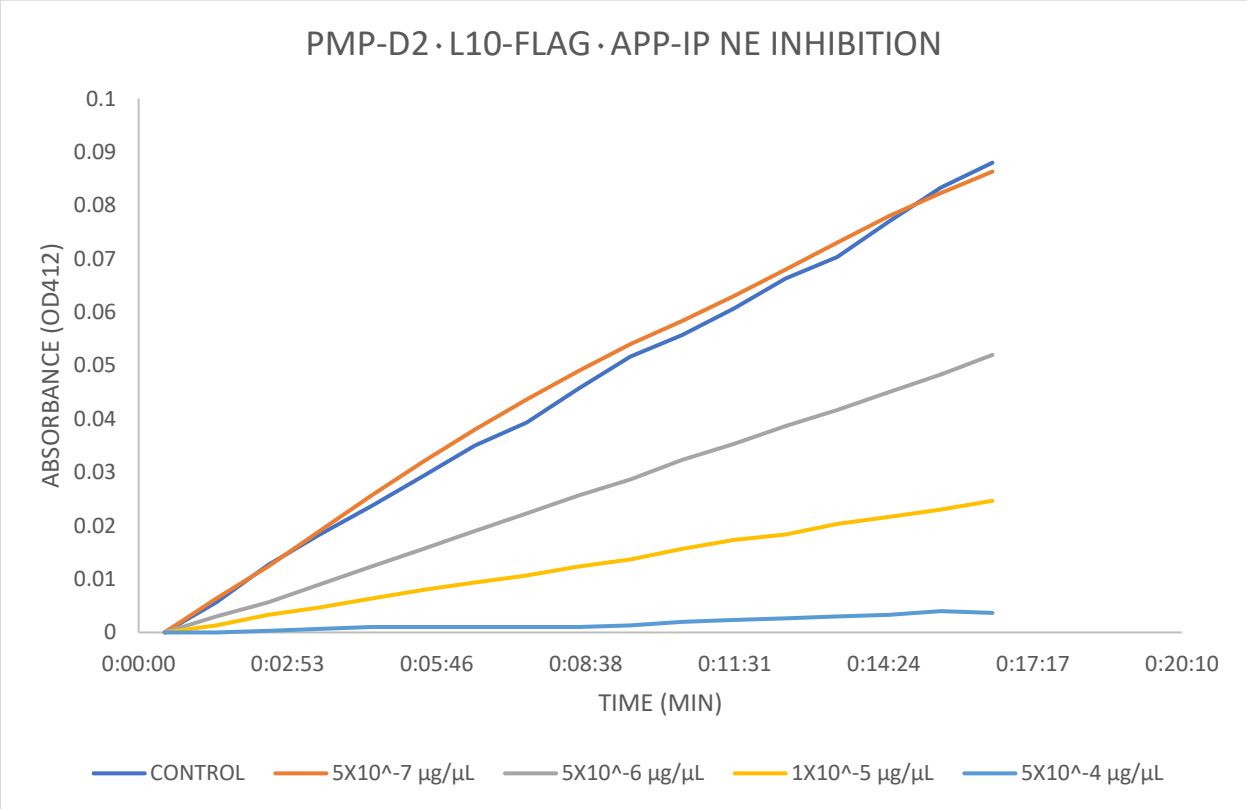

Figure 15 Kinetic Absorbance Measurements Over Time for the Various Concentrations of PMP-D2·L10-FLAG·APP-IP Providing Slopes Used to Indicate NE Inhibitory Activity

4.2.1 PMP-D2·L10-FLAG·APP-IP Compared to the Activity of the PMP-D2·L10-FLAG

It was predicted that PMP-D2·L10-FLAG would show inhibition activity against Neutrophil Elastase, which was in fact the observed result. Figure 16 shows the inhibition of NE by PMP-D2·L10-FLAG at the various tested concentrations. Similarly, PMP-D2·L10-FLAG·APP-IP showed the similar inhibitory activity at the same concentrations of PMP-D2·L10-FLAG indicating that the addition of APP-IP did not affect the NE inhibitory capabilities of the PMP-D2 region of the fusion protein PMP-D2·L10-FLAG·APP-IP. This result is observable when looking at the percent inhibition curves in Figure 19. The trendline indicates that the 50% inhibition for PMP-D2·L10-FLAG is $7.08x10^{-6}$.

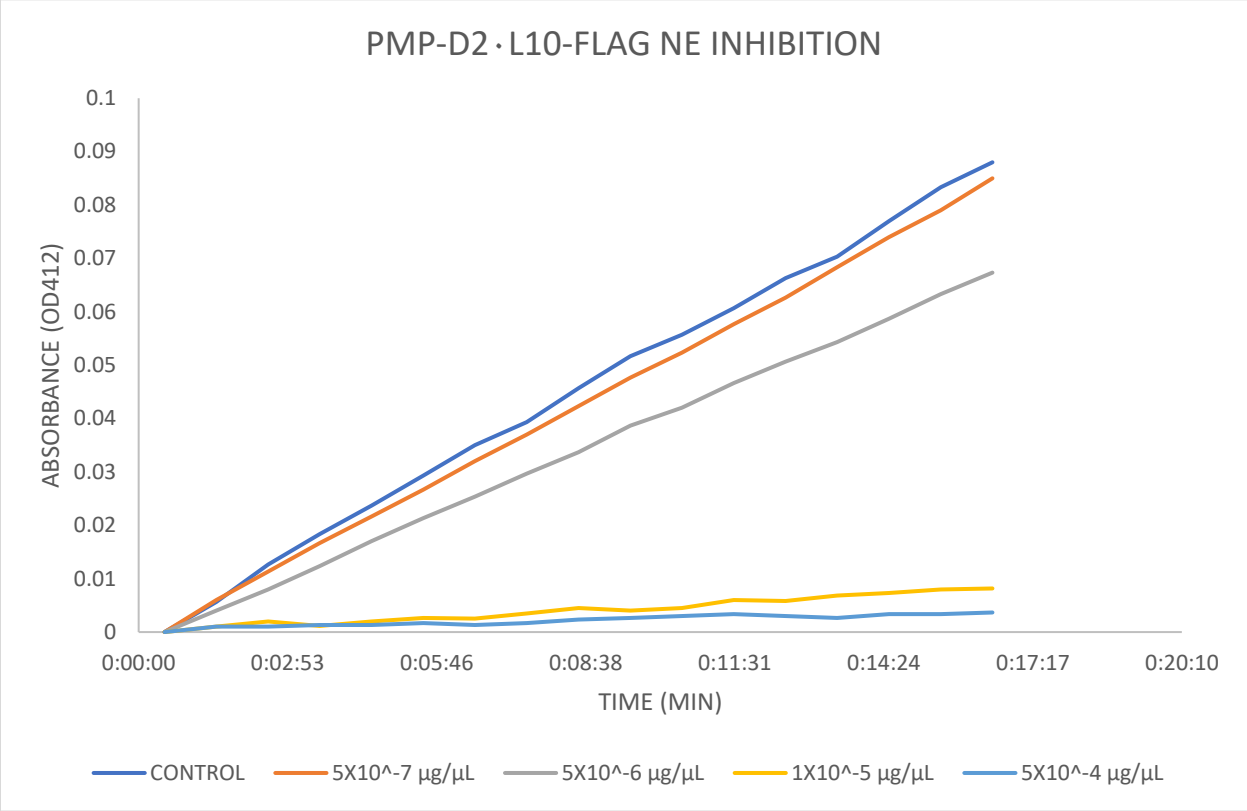

Figure 16 Kinetic Absorbance Measurements Over Time for the Various Concentrations of PMP-D2·L10-FLAG Providing Slopes Used to Indicate NE Inhibitory Activity

4.2.2 PMP-D2·L10-FLAG·APP-IP Compared to the Activity of APP-IP·L10-FLAG

In Figure 17 it is observed that no tested concentration of APP-IP·L10-FLAG inhibited Neutrophil Elastase to any substantial extent. In Figure 18 when comparing the logarithmic curves of APP-IP·L10-FLAG, PMP-D2·L10-FLAG, and the overarching fusion protein, PMP-D2·L10-FLAG·APP-IP, APP-IP·L10-FLAG was not a substantial contributor as it levels off at approximately 10% inhibitory capabilities at the highest tested concentration. On the contrary, PMP-D2·L10-FLAG and PMP-D2·L10-FLAG·APP-IP showed similar inhibitory capabilities, which indicates APP-IP did not subtract any substantial NE inhibitory activity. In fact, it is possible that it may contain some NE inhibitory capabilities, but no more than 10% in Figure 18.

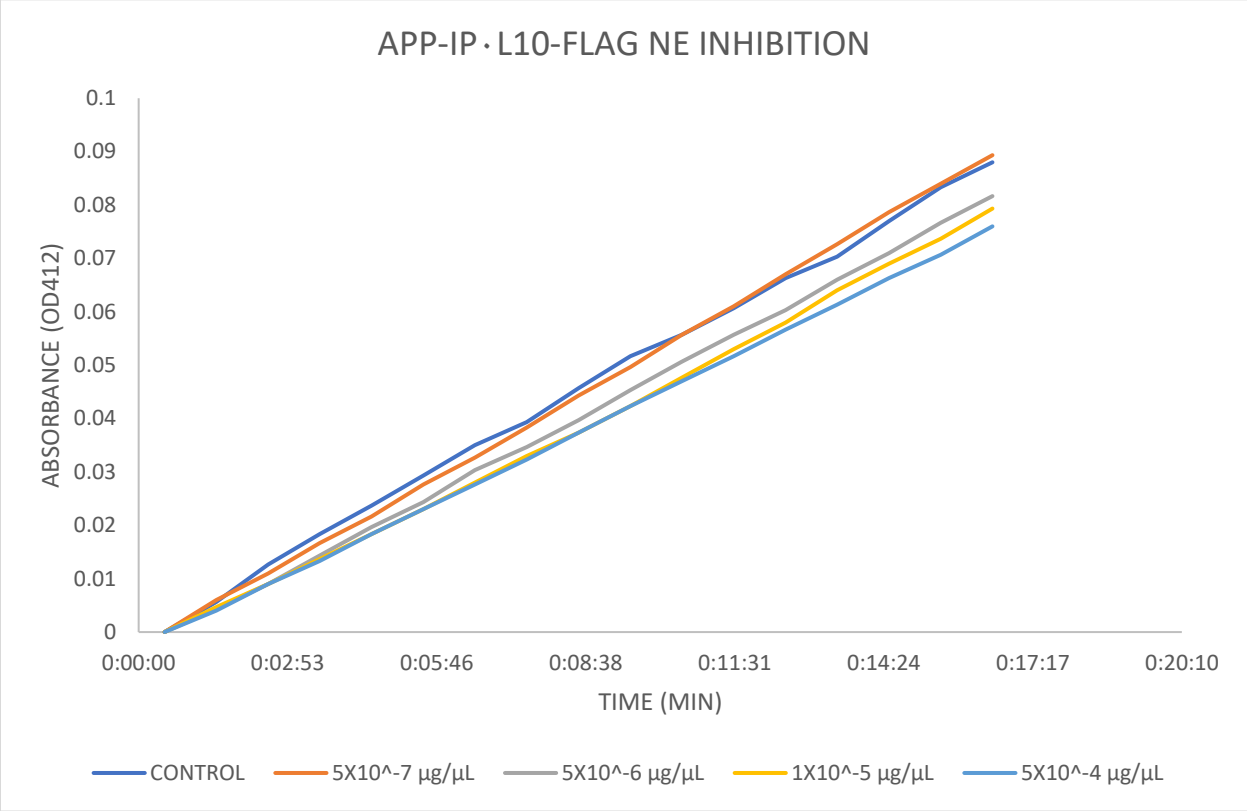

Figure 17 Kinetic Absorbance Measurements Over Time for the Various Concentrations of APP-IP·L10-FLAG Providing Slopes Used to Indicate NE Inhibitory Activity

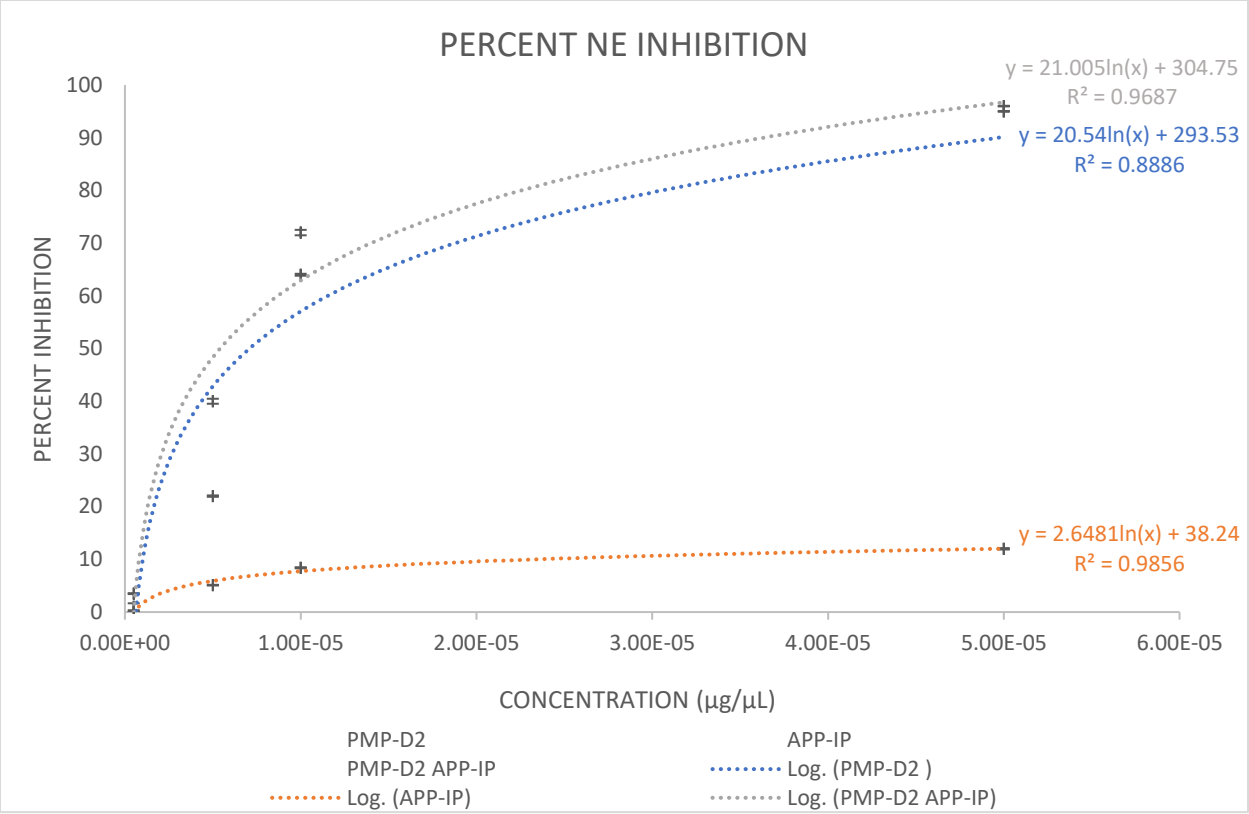

Figure 18 Percent NE Inhibition Gained from the Slopes of the Kinetic Readings Across Multiple Concentrations for the Experimental Groups

4.2.3 Statistical Significance of NE Inhibition Data

The statistical significance of the calculations of 50% inhibitory concentration is strong with $R^2 \geq 0.89$ indicating the trendlines used for the calculations of 50% inhibitory concentrations are a good fit. Also, percent standard error was found for the percent inhibition, which can be viewed on Figure 18**.** It can be observed that the standard error is very small. Furthermore, with a larger N, the standard error would decrease since the results seen are very repeatable with small standard error. Throughout the process of locating an array of inhibitory concentrations, for some concentrations there existed other data that is not included in order to keep N the same across all experiments. However, concentrations that were repeated and a second triplicate data set was found, the results were similar for percent inhibition.

CHAPTER 5: DISCUSSION

The results for MMP-2 inhibition and NE inhibition suggest that PMP-D2·L10-FLAG·APP-IP is a single molecule with dual functionality. This is proof of concept that fusion proteins can be built on an ELP platform with two biologically active peptide regions that maintain their unique biological activity. This is significant as this concept can be used by simple fusions of different peptides to ELPs to create a single molecule that is multifunctional rather than using a heterogeneous mixture of the peptides. Additionally, not only is PMP-D2·L10-FLAG·APP-IP multifunctional in its biological activity, but the L10-FLAG region provides a functionality that allows easy recombinant production and purification. Additionally, it provides a stable platform for biologically active proteins as they remain in aggregates in the site of application preventing fast washout of the protein that would be observed if small peptides like PMP-D2 and APP-IP were applied alone.

The isoelectric point proved itself necessary for obtaining aggregation during inverse transition cycling. Additionally, it can be inferred that with single charged fusions to ELPs, pI may be important to increase protein yield as even with single charged regions fused to an ELP will repel each other and decrease the number of protein molecules that can interact with each other reliant on the amount of repulsive force of the charged region of the protein of interest. This lends importance in increasing protein yield by increasing protein aggregation and decreasing protein loss throughout inverse transition cycling.

Additionally, preliminary data of an antimicrobial peptide built LL37‧L10-FLAG‧CECROPIN-A shows promise in obtaining synergistic effects by making a molecule containing two synergistic antimicrobial peptides. The left most image of Figure 19 displays a transformation of just a pET25b plasmid. The results show 61 colonies. The center image of Figure 19, which is LL37‧L10-FLAG pET25b transformed into BLR(DE3), shows 15 of colonies, which is much less than the pET25b plasmid transformation observed in the left image. However, in the far right image displayed in Figure 19, there are no colonies when LL37‧L10-FLAG‧Cecropin-A is transformed into BLR(DE3). This result suggests synergy between the two antimicrobial peptides bound to the same ELP backbone since the number of colonies tapers to zero when observing transformations of pET25b, LL37‧L10-FLAG pET25b, and LL37‧L10-FLAG‧Cecropin-A pET25b, respectively. Synergy cannot be completely confirmed without further testing after purifying the protein and running antimicrobial protocols with proper controls.

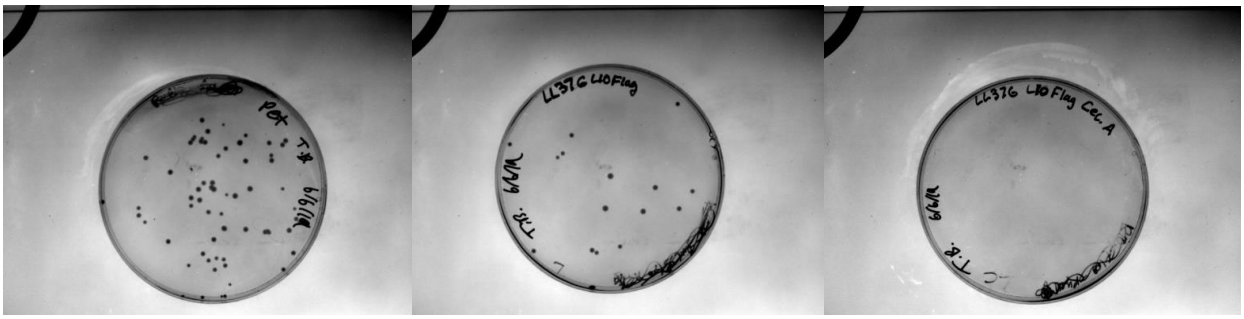

Figure 19 From Left to Right: pET25b, LL37‧L10-FLAG pET25b, LL37‧L10-FLAG‧Cecropin-A Transformed into BLR(DE3) E. coli Cells, Respectively.

LL37‧L10-FLAG shows antimicrobial activity and promise in obtaining the desired synergy which was the root directive for creating the molecule. It further confirms the ability to have multiple biologically active protein regions attached to and ELP backbone making a single molecule where the biological activities remain. There needs to be further research and experiments done to confirm synergy, however displaying activity is the first step to beginning

further experimentation to see if the attachment of two synergistic peptides to an ELP increases the antibacterial activity versus singularly attached antimicrobial peptides. There exist limitations to using well established antimicrobial protocol since the protein is insoluble and non-diffusible at 37°C. Additionally, like PMP-D2·L10-FLAG·APP-IP, this concept is not limited solely to synergistic interaction, but also gives insight on the ability to create similar antimicrobials with differing modes of action and differing targets to make single molecule a broad spectrum antimicrobial therapeutic. Furthermore, it could be advantageous to use an antimicrobial with a protease inhibitor on the same ELP backbone to make a protein that has activity for a broad array of biological processes or and antimicrobial with an anticoagulating protein for wound plugs. The possibilities are endless and as easy as "plug-and-play" to create single proteins with biological activity that is multi-characteristic.

CHAPTER 6: FUTURE STUDIES AND APPLICATIONS

With single molecule combination therapies on the forefront of research topics for treating complex diseases with complex factors, creating fusion peptides like PMP-D2·L10-FLAG·APP-IP and proving their effectiveness lends tremendous hope building on this concept. The future of these multifunctional fusion proteins lies in testing their effectiveness in animal models to observe whether the conclusion found in this work is also seen *in vivo*. Additionally, more research needs to be done on the behavior of these proteins *in vivo* in relationship to their transition temperatures. As seen in this research, an isoelectric point was needed to transition PMP-D2·L10-FLAG·APP-IP due to the charged ends of the molecule. As body pH can be dynamic in things like wounds or other diseases, it needs to be investigated that the fusion protein will transition in high concentrations despite the pH variations. However, even if it does not transition, it will still maintain diffusional properties that may be desirable for point specific applications since it is a large protein molecule.

Furthermore, studies must be done on the accumulative effect of the temperature and pH change on purified proteins' structures. It is well known that temperature, pH, and shear are the three factors that can denature proteins. By proposing pH changes throughout an already temperature dependent process, it is necessary to study possible alterations of the proteins' structures. The importance lies in the resulting protein solubility as denaturation can cause protein aggregates at room temperature, which may lead to protein loss during purification or loss of activity of the final protein yield. In respect to activity, an example could be the effect on

mechanisms that are mechanical by nature. Antimicrobial peptides rely on amphiphilic interaction with the amphipathic membranes of bacteria. Denaturation of antimicrobial fusion peptides may cause a loss of activity if the structural properties of the fusion proteins are greatly affected by denaturation due to pH and temperature changes throughout the purification cycles.

Future applications of this proof of concept are endless since there are peptides that exist that affect many proteinases, growth factors for tissue regeneration, or peptides for antimicrobial application, that can all be mixed and matched to create a single protein molecule with a "designer" multifunctional effect. Additionally, proteins could be easily adsorbed to the surface of polymers which in this case lends great value to implant devices. A multifunctional protein adsorbed to the surface of an implant device can provide the body with a designed immune response to the implant by creating a multifunctional protein that inhibits or induces certain responses of the immune system to the implanted material. Furthermore, using large ELPs as the backbone of these multifunctional proteins leads to the ability to create materials or stable coatings out of these fusion proteins as ELPs provide opportunity to cross-link the protein molecules together [1]. For example, this could provide applications like degradable wound plugs or hydrogels with antimicrobial and tissue regenerative effects for point specific application of open or closed wounds, where the bulk material is the therapeutic.

The ease of use of recombinant protein production using ELPs makes the applications numerous, and using them as a platform for the creation of a single molecule with multiple biological regions with specific biological effects makes their combination and point specific therapeutic effect valuable when compared the to pharmaceutical practices of mixing chemical compounds heterogeneously and systemically leading to side effects and drug interactions.

REFERENCES

[1] Atefyekta, S., Pihl, M., Lindsay, C., Heilshorn, S. C., & Andersson, M. (2019). Antibiofilm Elastin-like polypeptide coatings: functionality, stability, and selectivity. Acta Biomaterialia. https://doi-org.ezproxy.lib.usf.edu/10.1016/j.actbio.2018.10.039

[2] Marcos Heredero, Sandra Garrigues, Mónica Gandía, Jose F. Marcos, & Paloma Manzanares. (2018). Rational Design and Biotechnological Production of Novel AfpB-PAF26 Chimeric Antifungal Proteins. Microorganisms, (4), 106.

[3] McCarthy, B., Yuan, Y., & Koria, P. (2016). Elastin-like-polypeptide based fusion proteins for osteogenic factor delivery in bone healing. Biotechnology Progress, (4), 1029.

[4] Okonkwo, Uzoagu A., and Luisa A. DiPietro. "Diabetes and Wound Angiogenesis." International Journal of Molecular Sciences, MDPI, July 2017, www.ncbi.nlm.nih.gov/pmc/articles/PMC5535911/.

[5] Pourkavoos, N. (2012). Unique Risks, Benefits, and Challenges of Developing Drug-Drug Combination Products in a Pharmaceutical Industrial Setting. Combination Products in Therapy, 2(1), 1. Retrieved from

[6] van Hasselt, J. G. C., & Iyengar, R. (2019). Systems Pharmacology: Defining the Interactions of Drug Combinations. Annual Review of Pharmacology & Toxicology, 59, 21–40.

[7] Yu, G., Baeder, D. Y., Regoes, R. R., & Rolff, J. (2016). Combination Effects of Antimicrobial Peptides. Antimicrobial Agents and Chemotherapy, 60(3), 1717.